Journal of Materials Chemistry B

ROYAL SOCIETY OF CHEMISTRY

REVIEW

View Article Online
View Journal | View Issue

Check for updates

Cite this: J. Mater. Chem. B, 2026, 14, 12

Engineering polymeric micelles for targeted drug delivery: "click" chemistry enabled bioconjugation strategies and emerging applications

Enfal Civril, [a] Rana Sanyal *[ab] and Amitav Sanyal *[ab]

In recent years, there has been remarkable progress in designing drug delivery systems since the dawn of polymer therapeutics. Advances in polymer science and bioconjugation chemistry continue to advance the design and efficiency of drug delivery systems. Among the various drug delivery systems, polymeric micelles stand out because of their versatile features, like increased bioavailability of hydrophobic therapeutic cargo, as well as enhanced uptake in tumors because of their nanosize-mediated passive targeting. Importantly, the polymeric micelles can be engineered to actively target disease sites through surface functionalization with appropriate bioactive ligands. Decorating the micelle surface with bioactive ligands has emerged as one of the most preferred approaches to enhance their targeting capability. Over the years, many ligands have been explored for active targeting, ranging from sugars and peptides to antibodies and oligonucleotides. Progress in protein sciences and molecular biology continues to reveal new ligands and enlarge this library. Considering the delicate nature of the biological ligands, the utilization of mild, efficient, and benign chemical transformations is vital. In this context, the advent of "click" chemistry has dramatically altered the design of targeted micelles. The ability to modify polymers with "clickable" handles at the desired locations, as well as control over the density of these reactive units, expands the utilization of this chemistry. Over the years, the focus has shifted from the highly efficient copper-catalyzed azide–alkyne cycloaddition to "metal-free click" reactions. Additionally, bioorthogonal "click" reactions have enabled the achievement of "*in vivo* click" transformation-based targeting strategies either through metabolic glycoengineering or stimuli-induced aggregation. This review focuses on the advances in the fabrication of ligand-based targeted micelles using the "click" reaction for ligand conjugation onto polymeric micelles and highlights recent applications of these materials for targeted drug delivery.

Received 27th September 2025,
Accepted 11th November 2025

DOI: 10.1039/d5tb02193f

rsc.li/materials-b

Open Access Article. Published on 24 November 2025. Downloaded on 6/6/2026 1:27:29 AM.
This article is licensed under a Creative Commons Attribution-NonCommercial 3.0 Unported Licence.

1. Introduction

Drug delivery systems such as polymer–drug conjugates, hydrogels, nanogels, and micelles are emerging as promising platforms for healthcare applications.[1–15] Polymeric micelles are core–shell assemblies with sizes ranging from tens to hundreds of nanometers, usually obtained from the self-assembly of amphiphilic block copolymers in an aqueous environment.[16,17] Over the past two decades, these nanosized aggregates have attracted widespread interest in biomedical applications such as drug delivery, wound healing, and diagnostic imaging.[18–22] Their hydrophobic core can host a variety of hydrophobic therapeutically active drug molecules and thus solubilize them in an aqueous environment, as well as prevent their early metabolism in the biological milieu before reaching the disease site. Polymeric micelles offer solutions to common drawbacks of conventional therapies, such as low solubility of several drugs under physiological conditions, short half-life, rapid clearance, and high biodistribution, resulting in low bioavailability and decreased therapeutic outcome. Moreover, the polymer composition can be adjusted to avoid the immune system-mediated clearance by remaining in a stealth mode during circulation.[23,24] Apart from these attributes, micellar platforms can be tailor-made through chemical functionalization to tune release kinetics, stimuli-responsiveness, and allow modular modifications to facilitate targeted delivery.[25,26]

Even though it appears trivial, the size of these micelles has high significance in biomedical applications. Their size is leveraged as a 'passive' targeting strategy toward tumors or inflamed tissues. Size-selective accumulation in a tumor environment is achieved through the enhanced permeation

[a] Department of Chemistry, Bogazici University, Bebek, Istanbul, 34342, Turkiye, rana.sanyal@bogazici.edu.tr, amitav.sanyal@bogazici.edu.tr
[b] Bogazici University Center for Targeted Therapy Technologies, Istanbul, 34684, Turkiye

This journal is © The Royal Society of Chemistry 2026

Open Access Article. Published on 24 November 2025. Downloaded on 6/6/2026 1:27:29 AM.
This article is licensed under a Creative Commons Attribution-NonCommercial 3.0 Unported Licence.

and retention (EPR) effect that stems from disorganized epithelial cells in leaky vasculature and a weak lymphatic system.[27] Similarly, micelles can selectively accumulate in inflamed areas through extravasation through leaky vasculature and subsequent inflammatory cell-mediated sequestration (ELVIS) effect.[28] However, these effects help micelles to reach the diseased area rather than the specific disease cells. A targeting strategy that improves cellular recognition and internalization is necessary for selective uptake by cells. This strategy was first proposed by Paul Ehrlich almost a century ago, with the term ''magic bullet'' and is now commonly referred to as 'active' targeting.[29] This selective cellular recognition is usually achieved by incorporating targeting ligands ranging from small molecules such as sugars, vitamins, and peptides, to large biomolecules such as antibodies and aptamers, on the surface of micelles. These ligands can recognize specific receptors overexpressed on the target cells and help the internalization of micelles through receptor-mediated endocytosis. Ligand-mediated targeting helps to increase intracellular drug concentration, bioavailability, and therapeutic efficiency.[30] Such attributes enabling specific delivery becomes vital when it comes to cancer therapy due to the high toxicity of chemotherapy agents. Active targeting can also be employed to treat other diseases, such as inflammation and Alzheimer's through the utilization of suitable ligands. In the early years, sugars were widely explored as ligands for active targeting.[31,32] New receptors and ligands have come to light by advancing our understanding of the mechanisms and pathways for targeting diseases. The ligand library has also been growing with advances in high-throughput synthesis and screening technologies. Such advancements on several fronts continue to increase the interest of the scientific community in pursuing the utilization of polymeric micelles in fabricating targeted drug delivery systems.[30]

Targeted polymeric micelles can be fabricated in many ways; however, practical, facile, mild and scalable synthetic approaches are essential for clinical translation. Also of importance is ensuring the effective display of targeting ligands on the nanocarriers. Fortunately, the advances in polymer science allow one to obtain polymers with tailored composition, architecture and control over the placement of reactive handles for bioconjugations.[33–40] For ligand conjugation, maintaining the ligand's integrity after the reaction is crucial for efficient active targeting. This is even more important when working with fragile biomolecules like folded peptides and antibodies. Considering these factors, reactions with high efficiency, mild conditions, fast reaction kinetics, and without generation of

Enfal Civril

Enfal Civril received her undergraduate degree from the Department of Chemistry at Bogazici University, Istanbul, Türkiye. Thereafter, she obtained her MS degree in chemistry under the supervision of Prof. Rana Sanyal, working in the area of antibody-targeted therapeutics. Recently, Enfal obtained her doctoral degree in the Sanyal group, under the guidance of Prof. Rana Sanyal and Prof. Amitav Sanyal, working in the area of fabrication and application of polymer-based drug delivery systems, where she employed covalent and non-covalent approaches to engineer targeted nanosystems.

Rana Sanyal

Rana Sanyal graduated from Bogazici University with a BS degree in Chemical Engineering and continued her studies at Boston University, receiving her PhD degree in Chemistry. Prof. Sanyal started her career as a research scientist in Amgen Inc., California. Since 2004, she has been a faculty member at the Department of Chemistry at Bogazici University, Istanbul, Türkiye. Her current research interests focus on targeted drug delivery. Prof. Sanyal has been named one of the three Cartier Women's Initiative 2021 Global Science and Technology Pioneer Award fellows and the European Women Innovator in 2022. She is the director of the Bogazici University Center for Targeted Therapy Technologies, and is also the CoFounder and Chief Science Officer of RS Research, a clinical-stage biotechnology start-up developing novel nanomedicines.

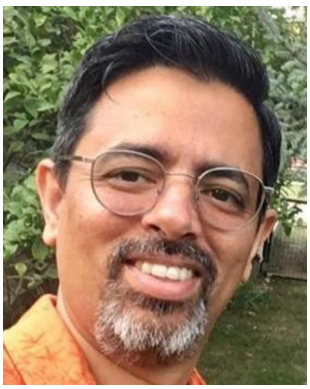

Amitav Sanyal

Amitav Sanyal obtained his undergraduate degree from the Indian Institute of Technology in Kanpur, India. He received his PhD from Boston University (USA), in the area of asymmetric organic synthesis. During postdoctoral work at the University of Massachusetts at Amherst, USA, he worked in the area of renewable polymeric coatings. Currently, he is a professor in the Department of Chemistry at Bogazici University, Istanbul, Türkiye. His research focuses on the design of novel polymeric materials such as coatings, hydrogels, polymeric micelles, and nanofibers for biomedical applications. His awards include the Young Investigator Award from the Turkish Academy of Sciences and from The Scientific and Technological Research Council of Türkiye, and he was elected as a Fellow of the Royal Society of Chemistry.

Open Access Article. Published on 24 November 2025. Downloaded on 6/6/2026 1:27:29 AM. This article is licensed under a Creative Commons Attribution-NonCommercial 3.0 Unported Licence.

toxic byproducts are in demand for conjugation. These requirements are fulfilled by a family of chemical transformations grouped under the umbrella of "click" chemistry.[41] Due to its versatile nature, "click" chemistry has found applications beyond drug derivery, from macromolecular synthesis to design of functional materials.[42–47] Because of these attractive assets, "click" reactions offer an effective approach to install ligands on micelles.[26,30] Ligand conjugation on micelles mediated through "click" reaction followed shortly after the paradigm of "click" chemistry was introduced.[48–53] Since then, a variety of "click" reactions have been used for bioconjugation of a range of bioactive ligands onto micelles. Most of the early reports of ligand attachment utilize the Huisgen-type copper-catalyzed azide–alkyne cycloaddition (CuAAC) "click" reaction.[53–58] However, toxicity concerns from the residual copper metal may compromise the efficiency of these systems. Metal-free "click" chemistry seamlessly integrates the power of "click" reaction with benign conditions needed for biological applications for ligand conjugations onto the micelles.[6,59–66] Within the metal-free "click" reactions, the highly efficient bioorthogonal transformations such as the strain-promoted azide–alkyne cycloaddition (SPAAC) and inverse electron demand Diels–Alder (IEDDA) are even suitable for "*in vivo* click"-based active targeting applications of micelles.

Although several reviews investigate the "click" reactions and drug delivery systems or micelles, this particular review focuses on the fabrication and application of targeted polymeric micelles that utilize "click" chemistry for ligand conjugation to engineer effective diagnostic and delivery platforms. Specifically, the review summarizes the attachment of ligands such as sugars, vitamins, peptides, small molecules, antibodies, antibody fragments, and aptamers. Apart from these ligands, "*in vivo*" active targeting strategies using micelles *via* metabolic glycoengineering and induced aggregation through bioorthogonal "click" reactions are also highlighted. In summary, this review aims to provide the reader with an overview of the use of "click" chemistry in the fabrication of targeted micelles and the utilization of *in vivo* "click" reactions for biomedical applications (Fig. 1). It is anticipated that by compiling and analyzing relevant strategies, this review will serve as a guidebook for researchers seeking to bioconjugate specific classes of targeting ligands onto micelles, while also showcasing a repertoire of design approaches to inspire the development of innovative and effective targeting systems for disease-specific applications.

2. Ligand targeted micelles: a general overview

The ability to deliver the therapeutic payload in a selective manner to the diseased cells is vital for drug delivery systems. This selectivity can be achieved by integrating specific ligands onto the carrier systems.[67,68] Ligands are unique molecules with a site-specific recognition ability and high binding affinity for their biomarkers or receptors. This feature of ligands can be

Fig. 1 Illustration of commonly employed "click" reactions to conjugate ligands onto micelles and types of ligands used for targeting. CuAAC: copper-catalyzed azide–alkyne cycloaddition, SPAAC: strain promoted azide–alkyne cycloaddition, IEDDA: inverse electron demand Diels–Alder.

employed to differentiate healthy and diseased cells since the unhealthy cells often overexpress specific receptors or biomarkers.[69] The most common ligands employed for achieving targeted drug delivery are carbohydrates, vitamins, peptides, proteins, antibodies, and oligonucleotides like aptamers, as summarized in Table 1.

Over the years, a tremendous amount of work has been reported about ligand-modified nanocarriers, including micelles, with a rich diversity of application arrays.[70–73] While the options for specific targeting ligands continue to expand, efficient conjugation chemistry has enabled reaching better outcomes for these smart carrier technologies.[18,68] The following part of the review will present examples of the fabrication of ligand-decorated micelles using "click" chemistry.

2.1 Carbohydrate-based targeting

Carbohydrates, commonly referred to as sugars, have been one of the most extensively studied ligands for targeted therapy due to their attractive properties, such as their intrinsic biocompatibility, and their important role in many biological pathways like signaling, adhesion, and recognition.[74,75] Additionally, as the "Warburg effect" suggests, carbohydrates play a role in cancer metabolism since cancer cells consume tremendous amounts of glucose and are consumed *via* fermentation, even in the presence of oxygen.[76–78] The enhanced need for sugar is leveraged to detect and target cancer cells with the help of

 This journal is © The Royal Society of Chemistry 2026

Open Access Article. Published on 24 November 2025. Downloaded on 6/6/2026 1:27:29 AM. This article is licensed under a Creative Commons Attribution-NonCommercial 3.0 Unported Licence.

Table 1 Survey of commonly employed ligands, receptors, advantages and disadvantages

Ligand	Example	Receptors	Advantages	Disadvantages
Carbohydrates	Monosaccharides, disaccharides	Lectin, asialoglycoprotein receptor (ASGPR), GLUT5 transporters, CD206, ricinus communis agglutinin	✓Biocompatible	✓Targeting and affinity variation
	Polysaccharides	Scavenger receptor class A (SR-A)	✓Naturally occurring molecules ✓Easy to functionalize, ✓Structural diversity	✓Decreased site-selectivity
Vitamins	Folic acid	Folate receptor (FR)	✓Small size, ✓Low cost, ✓Biocompatible, ✓Functionalizable acid group	✓Fast clearance from the body due to the existence of FR in the liver or plasma protein binding
	Biotin	Biotin receptors, avidin	✓Small molecule, ✓Biocompatible, ✓Easy to functionalize	✓Involves many cellular pathways, which may have decreased the site-specificity
Peptides	Tat, transferrin, Lyp-1, GE 11, F3, KTTKS, OA02, RGD *etc.*	Importin receptor, transferrin receptor, P32 protein, epidermal growth factor receptor (EGFR), nucleolin, PAR-2, α-3 integrin receptor, integrin, αvβ3 and αvβ5	✓Highly customizable, biodegradable, ✓Higher binding affinity and specificity than small molecule ligands, ✓Many functional groups for further functionalization	✓Poor stability, ✓High cost, ✓Short half-life, ✓Requires multiple steps to synthesize
Monoclonal antibodies (mAbs)	Anti-HER-2 antibody, trastuzumab, daratumumab, anti-CD276 antibody, cetuximab, anti-CD326 antibody	HER-2, CD38, CD276, EGFR, CD326	✓High sensitivity and specificity, ✓High purity, ✓Long serum life	✓High cost, ✓Difficulty in site-specific modification, ✓Strong binding causes delayed therapeutic effects, ✓May cause an immunogenic response ✓High molecular weight
Antibody fragments	Fab', single-chain variable fragment (scFv)	TF, stem cell antigen, EphA2 receptor	✓Smaller than mAbs, ✓Higher tumor penetration	✓Decreased half-life ✓Fewer available conjugation sites than mAbs may cause compromised binding affinity.
Oligonucleotides	Aptamers		✓High stability, specificity, and affinity, ✓Ease of functionalization, ✓Easy to synthesize and reproducible products ✓Low immunogenicity	✓Metabolic instability ✓High cost

radiolabeled sugars like fludeoxyglucose F18 (FDG) or by attachment of sugars to chemotherapy agents.[79,80] Later, it was discovered that by increasing the number of interactions of sugar molecules with their receptors, binding affinity was further enhanced, an effect termed as ''cluster glycoside effects.''[81–84] These findings increase the variability of constructs for sugar-targeted drug delivery systems. Increasing the multivalency can be accomplished in several ways, like incorporating them into polymer side chains, dendritic structures, or on the surface of micelles.[85–90] Scientists have studied various structural designs and conjugation chemistries to attach sugars to polymeric materials, including ''click'' chemistry-based approaches.[31,59,91–95] Within the scope of this review, it was noted that the CuAAC reaction and metal-free thiol–yne/ene ''click'' chemistries were among the most extensively explored methods for the conjugation of sugars onto micelles. Some select examples in this frame are discussed in detail; however, a diverse variety of examples are listed in Table 2.

The CuAAC ''click'' chemistry has been one of the most employed technique for conjugation of sugar onto micelles since the early 2010s. The sugar-coated micelles have been used for lectin binding, ricin inhibition, hepatocyte targeting, and developing drug delivery systems for cancer treatment.[55,96–103] The carbohydrate moeities have been conjugated to micelles from various positions like polymer end groups, polymer side chains, or dendron end groups to take advantage of the cluster glycoside effect by increasing the

Open Access Article. Published on 24 November 2025. Downloaded on 6/6/2026 1:27:29 AM. This article is licensed under a Creative Commons Attribution-NonCommercial 3.0 Unported Licence.

Table 2 List of carbohydrate-based ligands, type of "click" reactions used for conjugation, and applications

Ligand	"Click" reaction	Position of ligand	Targeting group	Cargo	Application	Ref.
Glucose	CuAAC	Chain end	N/A	N/A	Protein recognition (ConA)	96
Galactose	CuAAC	Side chain	N/A	N/A	Ricin inhibition	55
Glucose and maltose	CuAAC	Chain end	Lectin	DOX	Targeted cancer therapy	97
Glucose and maltose	CuAAC	Side chain	Lectin	DOX	Targeted cancer therapy	98
Glucose, lactose, and galactose	CuAAC	Chain end	Lectin	N/A	Targeted delivery system	99
Galactose	CuAAC	Chain end	ASGPR	pDNA	Hepatocellular carcinoma treatment	100
Mannose	CuAAC	Side chain	Lectin	DOX	Hepatocellular carcinoma treatment	101
Glucose	CuAAC	Chain end	Lectin	N/A	Targeted drug delivery system	102
Fructose	CuAAC	Chain end	GLUT5 transporters	Fluorescence probe C6	Breast cancer targeting	103
Glucose	CuAAC	Chain end	Lectin	N/A	Lectin binding	104
Mannose	CuAAC	Side chain	CD206	siRNA	Cancer therapy *via* tumor-associated macrophage targeting	108
Mono and disaccharide	CuAAC	Chain end	N/A	N/A	N/A	105
Glucose and fucose	CuAAC	Side chain	Fucose receptor	N/A	Targeted cancer therapy	110
Dextran	CuAAC	Hydrophilic block	SR-A	N/A	Rheumatoid arthritis (RA) treatment	106
Glucose and lactose	CuAAC	Dendron arms	Lectin	DOX	Targeted cancer therapy	120
Maltoheptaose	CuAAC	Chain end	Lectin	N/A	Protein recognition (ConA)	121
Galactose, glycopeptide	CuAAC	Side chain	Galactose-selective lectin RCA_{120}	N/A	Potential drug carriers for targeted therapy	112
Galactose & lactose, glycopeptide	CuAAC	Side chain	Lectin	N/A	Protein recognition (ConA)	113
Glucose and mannose, glycopeptide	CuAAC	Side chain	Lectin	N/A	Protein recognition (ConA)	114
Galactose and iminosugar, glycopeptide	CuAAC	Side chain	Sugar-binding enzymes	N/A	Glycosidase inhibition	116
Glucose and mannose, glycopeptide	CuAAC	Side chain	Lectin	Calcein and Nile red	Protein recognition (ConA), potential drug carriers for targeted therapy	115
Galactose, glycopeptide	CuAAC	Chain end	RCA_{120}	DOX	Hepatocellular carcinoma treatment	107
Galactose & lactose, glycopeptide	CuAAC	Side chain	Lectin	DOX & SPIO	Hepatocellular carcinoma treatment	117
Mannose	CuAAC	Side chain	Lectin	N/A	Protein recognition (ConA)	109
Glucose	Thiol–ene	Side chain	Lectin	N/A	Protein recognition (ConA)	50
Glucose	Thiol–yne	Side chain and Dendron arms	Lectin	N/A	Protein recognition (ConA)	130
Glucose	Thiol–yne	Side chain	Lectin	N/A	Protein recognition (ConA)	131
Glucose	Thiol–ene	Chain end	GLUT	N/A	Triple-negative breast cancer and glioblastoma targeting	59

Abbreviations: ASGPR: asialoglycoprotein receptor; N/A: not applicable; pDNA: plasmid DNA; RCA_{120}: ricinus communis agglutinin; SR-A: scavenger receptor class A.

multivalency. As an example of the polymer end group modification with sugars, Fort and colleagues reported amphiphilic glycoconjugates for lectin adhesion where lactose and *N*-acetylglucosamine ligands were conjugated to the hydrophilic extremity of micelles through the CuAAC "click" reaction.[104] Besides protein recognition, polysaccharides can be used as a targeting ligand to treat diseases such as rheumatoid arthritis, as explored by Park and coworkers, who designed polysaccharide functionalized micelles.[106] The amphiphilic block copolymer was obtained using the Huisgen-type 1,3-dipolar cycloaddition "click" chemistry between azide-terminated polycaprolactone (PCL) as the hydrophobic segment and alkyne-bearing dextran sulfate as the hydrophilic segment and targeting ligand for macrophage scavenger receptor class A (SR-A). The selective internalization of the micelles by activated macrophages was demonstrated, along with *in vivo* accumulation of the micelles at the inflammatory sites.

The most widely investigated application of targeted micelles, where carbohydrates are used as ligands, is for cancer therapy. In a recent example, Jan and coworkers reported

 This journal is © The Royal Society of Chemistry 2026

Open Access Article. Published on 24 November 2025. Downloaded on 6/6/2026 1:27:29 AM. This article is licensed under a Creative Commons Attribution-NonCommercial 3.0 Unported Licence.

glycopolypeptide-based targeted micelles for hepatocellular carcinoma treatment.[107] The saccharide lactobionolactone was functionalized with azide group and conjugated to terminal alkyne groups on the polypeptide poly(L-glutamic acid)-*b*-poly(L-phenylalanine) using the CuAAC "click" chemistry. This amphiphilic glycopolypeptide was self-assembled into a micelle while encapsulating DOX and displaying the targeting saccharide units on the surface of the micelle. Thus, sugar-targeted DOX-loaded micelles showed improved toxicity toward hepatocellular carcinoma cells compared to their non-targeted counterparts and free DOX.

Even though polymer end group modification contributes to the cluster glycoside effect when self-assembly occurs, increasing the multivalency of these carbohydrates may contribute further to increase the targeting efficiency. Conjugation of sugars to the polymer side chains is one way to achieve this, as demonstrated in a study by Giorgio and coworkers, where they designed mannose-decorated polymeric micelles for siRNA delivery to the macrophages, which overexpress CD206 mannose receptors (Fig. 2).[108] The conjugation of alkyne-modified mannose was performed after the polymer synthesis using the CuAAC "click" reaction with the azide pendant side chains. These micelles were selectively internalized by human macrophages and increased the siRNA delivery towards macrophages. Apart from ligand decoration for enabling active targeting, this example also demonstrates that micelles can be stimuli-responsive, tuning the cargo release using pH-responsive side chains in one of the blocks.

Stenzel and coworkers presented a different approach for conjugating sugars into polymeric scaffolds.[109] They synthesized a mannose glycomonomer using the CuAAC "click" reaction instead of performing post-polymerization conjugation. This monomer was homo-polymerized to obtain the hydrophilic segment of the micelle and further polymerized with NIPAAm to obtain a diblock amphiphilic copolymer. In an alternative approach, one of their later work employs the post-polymerization conjugation of sugars to polymer side chains using the CuAAC "click" chemistry.[110] A poly-(propargyl methacrylate)-*block*-poly(*n*-butyl acrylate) (PPMA-*b*-PBA) polymer was synthesized and functionalized with varying amounts of azide-terminated fucose and glucose. Obtained micelles were used as cancer-targeting drug delivery systems due to the upregulation of fucosylated proteins in multiple cancer types. It was established that the sugar-targeted micelles were internalized by lung, ovarian, and pancreatic carcinoma cells.

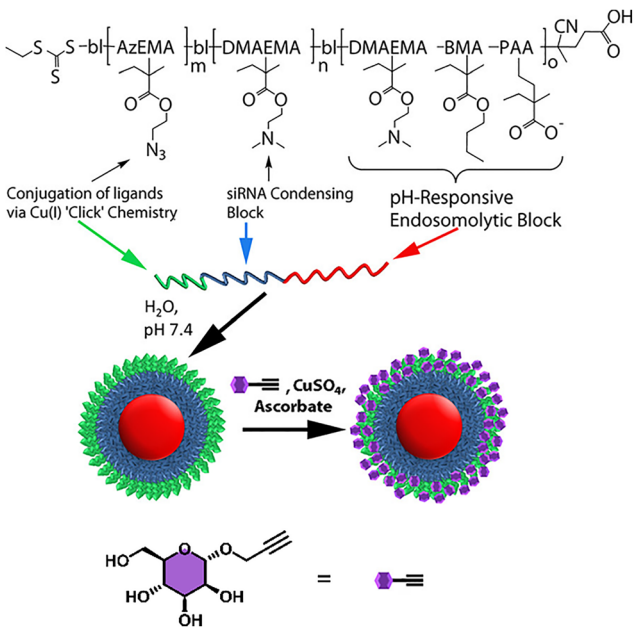

Fig. 2 The structure and schematic representation of the triblock copolymers, their micelle formation, and post-polymerization conjugation of targeting motifs to azide-bearing polymer side chains through CuAAC "click" reaction. Reproduced with permission.[108] Copyright 2013, American Chemical Society.

Conjugation of sugars to a polypeptide backbone has been employed for synthesizing glycopeptides.[111–114] Dhaware *et al.* reported a homo-glycopolypeptide where pendant alkyl chain-modified sugars were linked to the polymer backbone using the CuAAC reaction.[115] Thus obtained amphiphilic polymer self-assembled to yield micelles with binding affinity towards lectin Con A. Similarly, Lecommandoux and colleagues synthesized glycopolypeptide incorporated with iminosugars as inhibitors (Fig. 3).[116] A propargyl-modified synthetic polypeptide poly(*g*-benzyl-L-glutamate-*b*-DL-propargylglycine) was conjugated with azido-functionalized iminosugar using the CuAAC "click" reaction. The glycopolypeptide self-assembled in an aqueous environment to yield biomimetic nanoparticles with high glycosidase inhibition potency due to the multivalency of sugar ligands. Another nano-sized micellar construct using a diblock copolymer containing a hydrophilic sugar-conjugated poly(glutamate) block was reported by Jiang and colleagues.[117] A side chain azide-containing diblock copolymer, poly(3-caprolactone)-SS-poly(2-azidoethyl-L-glutamate) diblock copolymer was functionalized with alkyne-bearing galactose and lactose units using the CuAAC "click" reaction. The sugar-coated micelles were employed for simultaneous encapsulation of the anticancer drug DOX and superparamagnetic iron oxide nanoparticles as MRI agents. Obtained micelles increased internalization and better cytotoxic profile against hepatocellular carcinoma (HepG2) cells.

While one is able to achieve multivalent sugar display on the surface of the micelle through the utilization of diblock copolymers where one of the blocks contains multiple sugar units as side chain residues, the synthesis of such constructs can entail multistep synthesis. Thus, an alternative approach has been investigated where only the chain end of the polymer contains a sugar unit. Multiple polymeric chains on the surface of the micelle end up displaying the sugar units protruding out of the surface to interact with the biological receptors. Furthermore, employing dendritic structures allows the display of sugar moieties as clusters for increased binding efficiency. Several examples of micelles that utilize these design aspects have been reported.[118,119] An example of micellar constructs consisting of sugar-based ligands on dendritic scaffolds obtained using the CuAAC "click" reaction was reported by Dong and coworkers in 2011.[120] They polymerized caprolactone from a generation

Open Access Article. Published on 24 November 2025. Downloaded on 6/6/2026 1:27:29 AM.
This article is licensed under a Creative Commons Attribution-NonCommercial 3.0 Unported Licence.

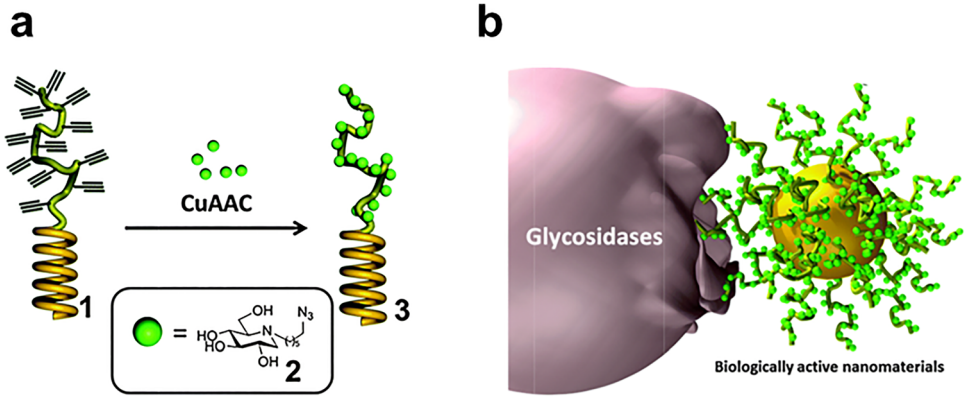

Fig. 3 (a) Schematic representation of alkyne pendant diblock polymer and azide functionalized sugar conjugation *via* CuAAC reaction to obtain glycopolypeptides, (b) illustration for the self-assembly of glycopeptides and their glycosidase inhibition. Reproduced with permission.[116] Copyright 2014, The Royal Society of Chemistry.

three poly(amidoamine) dendron bearing a propargyl group at the focal point, using ring-opening polymerization (ROP). Later, azide-functionalized sugar molecules are conjugated to the alkyne focal point of the G3 dendron to achieve active targeting of DOX-encapsulated self-assembled micellar nanoparticles. The authors demonstrate the affinity of the sugar-appended micelles towards lectins, Concanavalin A (Con-A), and Ricinus communis agglutinin. As an alternative, branched constructs can be used on the surface of the micelles to modulate binding efficiency, as demonstrated by Satoh and coworkers.[121] The authors studied the effect of the macromolecular architecture of miktoarm star polymers on their self-assembly and lectin binding. Using the CuAAC "click" reaction, alkyne pendant heptasugar polysaccharides were conjugated to azide group-terminated poly(caprolactone) (PCL) block. Among the various architectures evaluated, the 3-arm sugar-conjugated linear PCL polymer possessed the most significant interaction with ConA, suggesting the importance of cluster ligand presentation for effective biological recognition, an important feature for delivery systems.

As noted in the introduction, the CuAAC has been the most commonly employed "click" reaction to decorate micelles with targeting ligands. While the reaction offers many advantages, such as regioselectivity, chemical orthogonality, high reaction efficiency, and mild reaction conditions,[122–128] the use of copper metal may cause problems in the applications of these micelles due to the toxicity concerns that arise from the incomplete removal of copper metal. To address this problem, metal-free "click" reactions such as SPAAC, tetrazine-ene, thiol–ene and thiol–yne "click" chemistries have are gaining attention in polymer modification.[129] A metal-free conjugation strategy has been exploited by Stenzel and coworkers to fabricate sugar-targeted micelles where the sugar moiety was conjugated to the side chains of a polymer through the thiol–ene "click" reaction as a post-polymerization modification.[50] More than a single metal-free transformation could be utilized for the fabrication of targeted micelles, as demonstrated by Schacher and coworkers.[59] The authors fabricated worm-like core crosslinked micelles where the crosslinking was performed *via* Diels–Alder reaction and the surface functionalization for GLUT targeting was achieved by thiol–ene "click" chemistry between the allyl end groups of poly(ethylene oxide) and 6-thioglucose. These filomicelles were fluorescent since a Cyanine-5-based bismaleimide crosslinker was utilized for core crosslinking (Fig. 4). Obtained micelles were evaluated for cellular internalization in 2D and 3D cell cultures of MDA-MB-231 triple-negative breast cancer cells and U87MG glioblastoma cells. Using flow cytometry, the authors investigated the modulation of targeting efficiency with varying amounts of glycosylation. As expected, increased glycosylation led to higher cellular uptake, but only until a saturation point. The uptake efficiency was also tested on U87MG spheroids upon treatment with non-glycosylated and glycosylated filomicelles. Results show that increased penetration and uptake were seen for glycosylated micelles.

As mentioned before, the multivalent presentation of ligands plays an important role in biological recognition. As an example, Stenzel and colleagues investigated the effect of

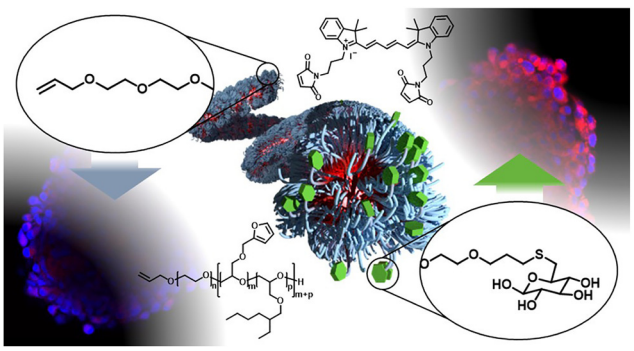

Fig. 4 Schematic representation of core-crosslinked filomicelles, sugar decoration *via* metal-free thiol–ene "click" reaction, and difference in uptake efficiency of non-targeted and targeted micelles by spheroids. Reproduced with permission.[59] Copyright 2021, American Chemical Society.

 This journal is © The Royal Society of Chemistry 2026

Open Access Article. Published on 24 November 2025. Downloaded on 6/6/2026 1:27:29 AM. This article is licensed under a Creative Commons Attribution-NonCommercial 3.0 Unported Licence.

branching on binding ability.[130] They designed micelles where one structure is composed of a diblock copolymer containing alkyne functionality at the side chains, whereas the other one is made from a dendron polymer conjugate where dendron ends are functionalized with an alkyne group. Thiol-containing sugar conjugation to both constructs was performed *via* radicalic thiol–yne ''click'' reaction. The number of sugar moieties on both constructs was kept similar to observe the effect of architecture on the binding ability of these micelles towards the Con-A. It was revealed that binding efficiency increased when sugars were oriented on the dendritic structure. As another example of side chain branching, Huang and coworkers designed an amphiphilic glycopolymer that self-assembled into micelles.[131] They conjugated thiol-bearing glucose molecules to the side chains of the polymer using the thiol–yne ''click'' chemistry. The densities of glucose molecules obtained using this approach were 37% and 58%. It was observed that the amount of glucose molecules on the micelles affects the aggregation and disaggregation behaviors with Con-A, since they affect the balance between hydrophobic–hydrophilic interactions.

The brief overview of sugar-based targeting ligands above highlights that sugars and polysaccharides are among the most extensively studied small-molecule ligands. Since sugars are one of the earliest studied targeting ligands, most examples utilize the CuAAC ''click'' reaction, while in more recent years the metal-free ''click'' chemistry examples have been employed. Also, one can expect that advances in glycochemistry will continue to expand and diversify the ligand library for targeting purposes. Other bioactive ligands, especially vitamins like folate and biotin, have gained attention as widely explored alternative targeting motifs.

2.2 Vitamin-based targeting

Vitamins are essential nutrient involved in many metabolic activities. Even though they adopt different roles depending on their type, some can be leveraged to target cancer cells because of the overexpressed receptors to which vitamins have high affinity.[132] In particular, vitamin B9 and B7, also known as folic acid and biotin, respectively, are among the most explored vitamin-based ligands for targeted therapy. The sections below highlight notable examples where ''click'' reactions have been employed to display vitamins as targeting ligands on the surface of micellar constructs.

2.3 Folic acid-based targeting

Folic acid (FA) is a subclass of vitamin B that participates in nucleotide base synthesis and cell proliferation. It can traverse the receptor-mediated endocytosis by anchoring to the folate receptor (FR). FA is a small molecule, has low cost, is non-immunogenic, and is stable over a wide range of temperatures and pH. Importantly, it can preserve its binding ability after conjugation with other molecules or drug delivery vehicles.[133] The utilization of FA with various nanostructures has been reported over the years.[134–142] As in the case of other ligands, conjugation of FA onto micelles can be accomplished through ''click'' chemistry.[60,143] Two common strategies stand out while examining the ''click'' conjugation of FA to the micelles: through the polymer side chains to increase the valency and to the polymer end groups either before or after micelle formation.

One of the earliest examples of conjugation of FA to the polymers *via* ''click'' chemistry in micellar structures was reported by Sumerlin and coworkers in 2008.[49] A block copolymer composed of *N*-isopropyl acrylamide (NIPAM), and *N*,*N*-dimethyl acrylamide (DMA) was synthesized using an azide functionalized chain transfer agent. A propargyl functionalized folate group was then attached to the polymer end group using the CuAAC ''click'' chemistry. Temperature-induced self-assembly yields micelles capable of controlled drug release. In a recent study, Wei and coworkers proposed a strategy for folic acid-decorated micelle formation without compromising the micelle integrity caused by the hydrophobicity of the folic acid.[144] They synthesized a redox-responsive miktoarm star-shaped amphiphilic copolymer PCL_3-SS-$POEGMA_1$ and modified the POEGMA terminus with an azide group. The FA was modified with a disulfide-bearing alkyne-containing linker. The conjugation of alkyne-SS-FA to the polymer was performed through the CuAAC ''click'' reaction. The competitive assay on the HeLa (human cervical adenocarcinoma) cell line confirmed cellular internalization through the FA receptor. Similarly, the cytotoxicities of targeted micelles with and without a competitive assay displayed a difference, supporting the receptor-mediated internalization. In another study, Zhang and colleagues reported a FA-targeted micelle for the delivery of DOX to cervical adenocarcinoma and breast cancer cells.[145] The authors synthesized a zwitterionic poly(ε-caprolactone) block poly(2-methacryloxoethyl phosphorylcholine) copolymer. Post-polymerization modification was performed to obtain the azide group at the polymer chain end. Propargyl-functionalized FA was conjugated to the polymer using the CuAAC ''click'' chemistry. DOX-loaded FA-targeted micelles showed enhanced internalization and improved cytotoxicity profile against HeLa and MCF-7 cell lines.

There are also several other examples where FA was conjugated to polymer side chains *via* a ''click'' reaction.[56,146,147] Liu and coworkers reported unimolecular micelle for targeted drug delivery and MR imaging.[56] The micelle-forming polymer (H40-PCL-*b*-P(OEGMA-*co*-AzPMA)) was obtained from the sequential polymerization of ε-caprolactone and a copolymer of OEGMA and 3-azidopropyl methacrylate (AzPMA) on the periphery of a hyperbranched polyester H-40. The azide side chains were modified with alkyne-containing gadolinium (Gd) complexed DOTA and propargyl functionalized FA using the CuACC ''click'' chemistry. In another related work, instead of the unimolecular micelle, the authors designed a mixed polymeric micelle system using PCL-*b*-P(OEGMA-FA) and PCL-*b*-P(OEGMA-Gd) polymers, where the same methodology as their previous work was used to conjugate FA and DOTA-Gd.[148] Paclitaxel encapsulated mixed micelle was toxic against HeLa cells, whereas the empty micelle was non-toxic. *In vivo* MR imaging displayed enhanced signal intensity and improved

Open Access Article. Published on 24 November 2025. Downloaded on 6/6/2026 1:27:29 AM. This article is licensed under a Creative Commons Attribution-NonCommercial 3.0 Unported Licence.

accumulation. In a subsequent study, the authors further improved the system by incorporating shell-crosslinking through slight modifications on the polymers.[149] One of the polymers was conjugated with the chemotherapy agent camptothecin (CPT) using the CuAAC "click" chemistry.

Song *et al.* reported a polyurethane-based micelle obtained from biodegradable poly(ε-caprolactone) (PCL), L-lysine ethyl ester diisocyanate (LDI), redox-responsive disulfide bond and clickable alkyne groups (Cys-PA) containing chain extender, and hydrophilic PEG chain *via* pH-sensitive benzoic–imine linkage (BPEG).[150] The targeting ligand FA was conjugated to the side chains *via* CuAAC "click" reaction. DOX-loaded targeted micelles displayed high cellular internalization and an enhanced cytotoxicity profile. Their follow-up work also uses a similar strategy with slight modifications to the polymer.[146] The authors increased the number of alkyne groups on the polymer's side chain, which increases the number of FA groups. Besides DOX, superparamagnetic iron oxide nanoparticles (SPION) were also loaded into the micelles to serve as MRI contrast agents and magnetically-guided MR imaging for theranostic applications. Cheng *et al.* synthesized an amphiphilic copolymer using post-polymerization modification of pendant azide groups of the poly(epichlorohydrin) (PECH-azide) polymer with the monopropargyl-modified linear PEG and alkyne-modified FA *via* CuAAC "click" reaction (Fig. 5).[151] Obtained F-PECH-PEG polymer could self-assemble into polymeric nanoparticles with a small size of around 30 nm. Internalization of the DOX-loaded FA-targeted particles was higher than that of the non-targeted ones in cancer cells.

Despite the toxicity concerns of CuAAC chemistry in biological applications, FA conjugation to micelles *via* metal-free "click" reaction is still rare. Utilization of the thiol–maleimide "click" reaction for the synthesis of FA-targeted micelle was reported by Gong and coworkers.[51] The authors synthesized poly(*N*-vinyl caprolactam)-*block*-poly(ethylene glycol) diblock copolymer, where the PEG chain end group was modified with a maleimide group to conjugate FA-SH. Blank and 5-FU loaded FA-targeted micelles did not exert high cytotoxicity towards the healthy cells, yet drug-loaded targeted ones exhibited toxicity towards the mouse mammary carcinoma cells.

As shown in above examples, advances in synthetic polymer science enables engineering systems amenable to undergo conjugation with various types of targeting ligands, such as folic acid. Although folic acid is one of the most explored targeting ligands, its combination with micelles through "click" reaction is limited. Among the limited examples, the CuAAC "click" chemistry is predominant, while metal-free "click" chemistry has been rarely reported. Nonethless, considering the advantages that folic acid based targeting offers, one can anticipate that such systems will witness further developments.

2.4 Biotin-based targeting

Biotin functions as a coenzyme and promotes cell growth, aiding many other functions like maintaining blood sugar levels, bone marrow health, and biological reactions.[70,72] The biotin receptors are elevated in many cancer cells due to the high biotin consumption by the cancer cells to continue their uncontrolled growth.[132] These aspects make biotin a good candidate for targeting ligands, and it has been incorporated into many carrier systems, including micelles.[152–155] Various conjugation strategies have been examined to install biotin onto carrier systems, including "click" reactions.[156–158] Biotin can be integrated at the chain end of a polymer or as pendant side chain residues. For example, Thayumanavan and coworkers reported biotin conjugation to micelles using the CuAAC "click" reaction as an example of polymer end group modification.[54] They designed dendritic micelles that undergo protein-binding-induced disassembly and used biotin as a ligand for specific interaction with a protein. It was observed that the disassembly of micelles induced by the interaction of biotin with avidin resulted in the release of the encapsulated cargo.

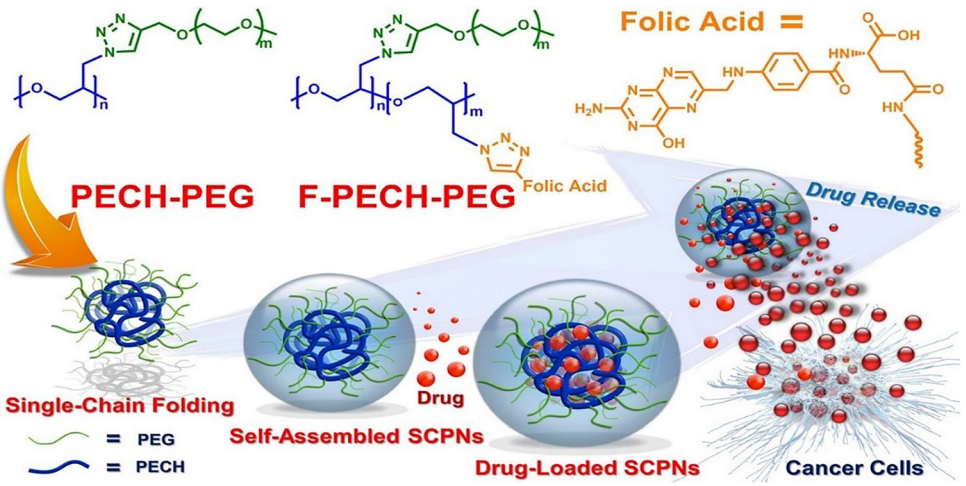

Fig. 5 Schematic representation of FA conjugated micelles, drug loading, and release processes. Reproduced with permission.[151] Copyright 2021, American Chemical Society.

 This journal is © The Royal Society of Chemistry 2026

Open Access Article. Published on 24 November 2025. Downloaded on 6/6/2026 1:27:29 AM. This article is licensed under a Creative Commons Attribution-NonCommercial 3.0 Unported Licence.

As another example, Fang *et al.* fabricated polymeric micelles for sensing and calorimetric detection applications.[159] The system was composed of amphiphilic block polymer biotin-labeled poly(ethylene glycol)-*block*-poly(3-acryl aminophenyl boronic acid), where the biotin was conjugated using Huisgen type ''click'' reaction. Likewise, Doris and coworkers designed a micelle for targeting breast cancer where the targeting ligand biotin was conjugated to the micelle surface through the CuAAC ''click'' reaction.[160] They demonstrated that the internalization of micelle was increased with the presence of biotin as a ligand, and the role of biotin in internalization was established through a competitive assay, which resulted in decreased internalization. Similarly, micellar systems for gene delivery have been explored by Weberskirch and coworkers by using a biotin-clicked micelle for active targeting.[161]

Zhao and colleagues chose to conjugate biotin to the side chains of the polymers.[52] Their first work reported a micelle formation from the azido-containing amphiphilic triblock copolymer poly(ethylene glycol)-*b*-poly(azidoethyl methacrylate)-*b*-poly(methyl methacrylate) (PEG-*b*-PAzEMA-*b*-PMMA). Upon self-assembly of PEG-*b*-PAzEMA-*b*-PMMA, azide groups are presented at the interface of hydrophilic and hydrophobic blocks. Biotin was conjugated to azide side chains through the CuAAC ''click'' reaction after the micelle formation. The avidin binding ability was shown *via* avidin/HABA competitive binding assay. Their latest work along this concept reports the synthesis of a triblock copolymer where the junction points of the blocks were functionalized with alkyne groups.[162] Post-micellization modifications were done using the CuAAC ''click'' reaction between the pendant alkyne units and biotin-azide.

Biotin is a promising targeting ligand candidate due to its biocompatibility and the overexpression of the biotin receptor on many cancer cells. It can be functionalized in many ways; however, its use with micelles through a ''click'' reaction is predominantly limited to the CuAAC ''click'' reaction. The use of biotin as a targeting ligand with micelles through a ''click'' reaction can be further improved by considering other ''click'' reactions, given the wide range of application areas. Although vitamins offer advantages over sugars, they are also widely distributed in the body as they are involved in many biological pathways. This may result in the broad biodistribution of vitamin-decorated carriers, causing off-target delivery and low bioavailability of therapeutic agents. Therefore, larger and more specific ligands, such as peptides, have been extensively explored for improved targeting.

2.5 Peptide-based targeting

Peptides are a particular class of ligands, smaller than antibodies but larger than other small-molecule ones. They can offer high binding affinity and specificity towards their receptors. Moreover, they can target specific sites in many diseased areas, including cancer, Alzheimer's, or inflamed areas, as well as cross biological barriers, such as the blood-brain barrier. Additionally, they can be engineered to possess many functional groups at a particular location and are available for further modifications to enable bioconjugation.[163–165] All these properties make peptides an attractive choice for targeting ligands. As the peptide library with targeting capability grows, its combination with many constructs, such as polymer brushes, metal complexes, nanoparticles, and micelles, has garnered increased interest over the years.[166–174] There are various strategies to tether them with drug delivery systems covalently, and ''click'' chemistry has been one of the most employed reactions in recent years.[175,176] This section of the review will focus on the micelles decorated with peptides through ''click'' chemistry. Even though some examples are discussed in detail, an exhaustive list is presented in Table 3.

Frequently peptides have been modified to contain an alkyne or azide group to enable their conjugation onto micelles using the CuAAC ''click'' reaction.[57,177–181] For example, Vagner and coworkers fabricated a targeted micelle by the conjugation of an alkyne-modified peptide 4-phenylbutyryl-His-DPhe-Arg-Trp-Gly-Lys(hex-5-ynoyl)-NH_2 to an azide decorated micelle.[57] This ligand has demonstrated selective binding to human melanocortin 1 receptor (hMC1R), overexpressed in melanoma. Both targeted polymer and micelle were shown to be selective against the receptor and maintained the binding affinity of the peptide after the ''click'' conjugation. In another study, Xiao *et al.* investigated the OA02 peptide-targeted micelles against ovarian cancer, where the alkyne-modified peptide was reacted with azide-terminated PEG5K-CA_8 telodendrimer using the CuAAC ''click'' reaction.[179] This formulation showed better antitumor efficacy than its non-targeted counterpart *in vivo*. Similarly, Zhang and colleagues fabricated polypeptide micelles decorated with nuclei targeting Tat peptide using the CuAAC ''click'' reaction.[180] The tumor targeting efficiency was further promoted by targeting nuclei through the Tat peptide, which was activated after cellular internalization at lysosomal pH. While shielding the encapsulated drug within the micelle during circulation to evade systemic toxicity is essential, accomplishing efficient intracellular drug release is equally crucial for micelle efficacy. Endogenous stimuli furnish an encouraging mechanism to trigger drug release through the cleavage of drug–polymer bonds or the disintegration of the micelle. In this context, Jiang and coworkers designed reactive oxygen species (ROS) responsive polymeric micelles against the early target for Alzheimer's disease (AD).[181] Their system was composed of an amphiphilic diblock copolymer of PEG-LysB. The amine groups of lysine were functionalized with pinacol phenylboronic ester to introduce hydrophobicity and ROS-responsiveness. Azide terminated PEG-LysB (N_3-PEG-LysB) was utilized to install a receptor for advanced glycation end-products (RAGE) targeting peptide (Ab) *via* CuAAC ''click'' reaction. *In vitro* and *in vivo* studies showed that this system could modulate the microglia activity and trigger neuroinflammation inhibition in the early stages of AD.

The ligand density on the micellar construct plays an important role in its efficient cellular uptake, and up to a certain level, increasing the ligand density can provide more efficient targeting capability. In this context, Stenzel and coworkers reported a core-crosslinked micelle decorated with different densities of tumor necrosis factor-related apoptosis-inducing

Open Access Article. Published on 24 November 2025. Downloaded on 6/6/2026 1:27:29 AM.
This article is licensed under a Creative Commons Attribution-NonCommercial 3.0 Unported Licence.

Table 3 List of peptide-based ligands, type of "click" reactions used for conjugation, and applications

Peptide	"Click" reaction	Position of ligand	Target molecule	Cargo molecule	Application	Ref.
CKR and EVQ	CuAAC	Chain end	FLT3	CUR	Leukemia treatment	177
His-D-Phe-Arg-Trp-Gly-Lys	CuAAC	Chain end	hMC1R	N/A	Melanoma targeting	57
OA02	CuAAC	Chain end	α-3 integrin receptor	PTX	Ovarian cancer treatment	179
Tat Nuclear localization signal (NLS)	CuAAC	Chain end	import receptors importin α & β Nuclear targeting	DOX	Cervical cancer treatment	180
KLVFFAED	CuAAC	Chain end	RAGE	CUR	Alzheimer's disease treatment	181
TRAIL-mimicking peptide, cyclized WDCL	CuAAC	Chain end	Death receptor 5	N/A	Colon cancer treatment	182
Transferrin	Thiol–maleimide	Chain end, after micelle formation	Transferrin receptor	PTX	Glioma treatment	183
TTGNYKALHPHNG	Thiol–maleimide	Chain end	BBB	DNA	Brain-targeted gene delivery	184
CGYGPKKKRKVGG (NLS)	Thiol–maleimide	Chain end	Importin α & β	DOX	Nasopharyngeal epidermoid carcinoma treatment	140
CGNKRTRGC (Lyp-1)	Thiol–maleimide	Side chain, after micelle formation	P32 protein	DTX and IR820	Breast cancer treatment	185
KDEPQRRSARLSAKPAPPKPEPKPKKA-PAKKC (F3 peptide)	Thiol–maleimide	Chain end	Nucleolin	PTX	Breast cancer treatment	186
YHWYGYTPQNVI (GE 11 peptide)	Thiol–maleimide	Chain end	EGFR	DOX and CEL	Triple-negative breast cancer	187
KTTKS	Thiol–maleimide	Side chain, after micelle formation	PAR-2	CUR	Wound healing	61
GIRLRG	Thiol–ene	Side chain, after micelle formation	GRP78	PTX	Breast cancer treatment	188
CREDVW	Thiol–ene	Chain end	Endothelial cells	ZNF580	Gene transfer for rapid endothelialization of artificial blood vessels	189
P18-4	Schiff base	Chain end	Cell surface receptors	N/A	Breast cancer treatment	190
Melanoma antigen peptides (GP100 and TRP 2), T-helper peptide (PADRE), dendritic cell targeting peptide (CLEC9A)	SPAAC	Branched chain ends	T-cells	N/A	Nanovaccine against melanoma	191
KGRGDS	CuAAC	Chain end, after micelle formation	Integrin, αvβ1	N/A	Wound healing, eye injury	53
RGGPLGVRGDG	CuAAC	Between the hydrophilic and hydrophobic blocks	Integrin, αvβ3 and MMP	PTX	Targeted cancer therapy	203
cRGD	CuAAC	Side chain	Integrin, αvβ3	CPT	Liver cancer treatment	204
cRGD	Thiol–maleimide	Chain end	Integrin, αvβ3	DTX and CA4	Ovarian cancer	15
cRGD	Thiol–maleimide	Chain end	Integrin, αvβ3	PTX	Glioblastoma treatment	205
cRGD	Thiol–maleimide	Chain end	Integrin, αvβ3, αvβ5	DACHPt	Glioblastoma treatment	206
cRGD	Thiol–maleimide	Chain end	Integrin, αvβ3	DOX	Glioblastoma treatment	207
cRGD and angiopep-2	Thiol–maleimide	Chain end	Integrin, αvβ3 and LRP1	DOX	Glioma treatment	208
RGD	Thiol–maleimide	Chain end	Integrin	Bar, or Oct, or Sal, or Pra	Autosomal dominant polycystic kidney disease treatment	62
cRGD	Thiol–ene	Dendrimer end groups	Integrin, αvβ3	DOX	Targeted cancer therapy	209
cRGD	Thiol–ene	Chain end	Integrin, αvβ3	DOX	Breast cancer treatment	210
RGD	SPAAC	Chain end, after micelle formation	Integrin, αvβ3	7-ethyl CPT	Breast cancer treatment	211

Abbreviations: Bar: bardoxolone methyl; BBB: blood-brain barrier; CPT: camptothecin; CEL: celecoxib; CUR: curcumin; DACHPt: (1,2-diamino cyclohexane) platinum(II); DOX: doxorubicin; EGFR: epidermal growth factor receptor; FLT3: feline McDonough Sarcoma like tyrosine kinase 3; hMC1R: human melanocortin 1 receptor; GRP78: glucose-regulated protein 78; LRP1: low-density lipoprotein receptor-related protein-1; Oct: octreotide; Pra: pravastatin; PTX: paclitaxel; RAGE: receptor for advanced glycation end-products; Sal: salsalate.

This journal is © The Royal Society of Chemistry 2026

Open Access Article. Published on 24 November 2025. Downloaded on 6/6/2026 1:27:29 AM.
This article is licensed under a Creative Commons Attribution-NonCommercial 3.0 Unported Licence.

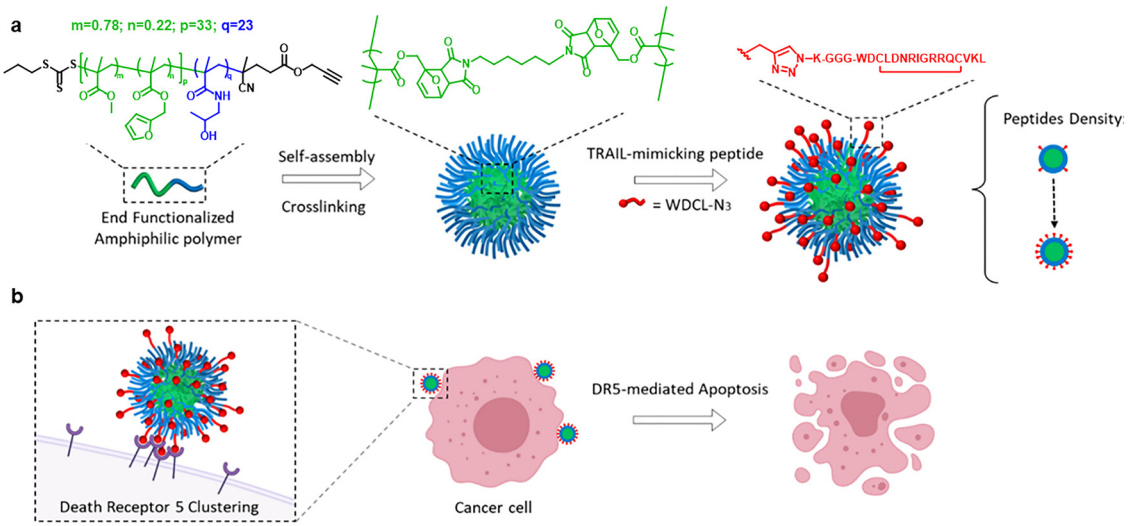

Fig. 6 Illustration of micelle preparation and mechanism of action. (a) Structures and reaction schematic of the amphiphilic polymer, micelle formation *via* self-assembly, core-cross-linking, and peptide attachment by CuAAC "click" reaction. (b) Micelles with multivalent TRAIL-mimicking peptides on the surface induce cancer cell apoptosis through DR5 clustering. Reproduced with permission.[182] Copyright 2023, American Chemical Society.

ligand (TRAIL) mimicking peptide.[182] They employed the Diels–Alder "click" reaction for core crosslinking and the CuAAC "click" reaction for the conjugation of the targeting peptide (Fig. 6). The authors investigated the effect of peptide density on death receptor-driven apoptosis since increasing the valency of ligands promotes receptor aggregation, leading to amplified signal and apoptosis. Within the various peptide densities, micelles with a 15% peptide density show the best activity against the colon cancer cell line, with an IC_{50} value of 0.8 μM.

Apart from the CuAAC "click" reaction, other "click" chemistries have also been investigated for peptide conjugations. As an attractive alternative, metal-free "click" chemistry has raised much interest since many of these reactions proceed with high efficiency under mild conditions without toxic byproducts or reagents. The thiol–Michael addition reaction falls into this category due to the high reactivity of thiol groups and facile introduction of the reactive counterparts into macromolecular constructs like polymers or peptides. These attributes make the thiol–maleimide dyad one of the most explored metal-free "click" reactions for peptide conjugation onto micelles.[37,61,183–187] As one of the early reports, Zhang *et al.* fabricated transferrin-conjugated polyphosphoester hybrid micelles against glioma.[183] Surface decoration with transferrin was achieved *via* the thiol–maleimide "click" reaction. Paclitaxel-loaded targeted micelles display improved cellular internalization *in vitro* and enhanced survival rate *in vivo*. In another report, Yu *et al.* designed a dual-targeted polymeric micelle system against human nasopharyngeal epidermoid carcinoma.[140] They fabricated cholesterol-modified glycol chitosan and functionalized it with FA and nuclear localization signal (NLS), a particular peptide sequence recognized by nuclear transport proteins. While FA was conjugated through a coupling reaction, NLS was attached using the thiol–maleimide "click" reaction. DOX-loaded dual-targeted micelles displayed the highest cytotoxic effect against human nasopharyngeal epidermoid carcinoma cells. *In vivo* studies support the targeting specificity of DOX-loaded dual-targeted micelles and improve the antitumor efficiency of DOX. Sun and colleagues reported a paclitaxel-carrying micelle system for targeting breast cancer.[186] Maleimide-functionalized PEG-PLA micelle was decorated with nucleolin binding peptide F3 *via* thiol–maleimide "click" reaction. *In vitro* and *in vivo* studies revealed enhanced accumulation and toxicity upon targeted micelle treatment compared to non-targeted counterparts. Sanyal and coworkers recently reported a cRGD-targeted micelle obtained from the reaction of maleimide-conjugated PEG–PLA and thiol-bearing cRGDfC peptide using the thiol–maleimide "click" reaction. This micellar system was designed to deliver DTX and CA4 simultaneously, and it was shown to be toxic against SKOV-3 ovarian cancer cells.[15] Similarly, Li and coworkers developed an epidermal growth factor receptor (EGFR) targeted micelle system to deliver Celecoxib (CEL) and DOX against metastatic breast cancer.[187] Maleimide functionalized PEG was polymerized with trimethylene carbonate (TMC) *via* ROP to obtain an amphiphilic diblock copolymer Mal-PEG-PTMC, and DOX was conjugated post-polymerization. GE11, a peptide with a high affinity for EGFR, was introduced using the thiol–maleimide "click" reaction to yield GE11-P-DOX. Encapsulation of CEL yields EGFR-targeted dual-drug carrier micelles. This targeted micelle displays enhanced tumor accumulation and cellular uptake. The *in vivo* studies revealed a high tumor inhibition rate and lung metastasis inhibition upon administering these targeted micelles. Recently, Kim and colleagues fabricated a targeted micelle for wound healing applications.[61] Their polymeric nanosystem was composed of a mixture of poly(ethylene oxide)-*block*-poly(ε-caprolactone) (PEO-*b*-PCL) and a mannosyl erythritol lipid (MEL)–maleimide linker (Fig. 7). To achieve selective fibroblast targeting, the proteinase-activated receptor (PAR-2), which is present

Open Access Article. Published on 24 November 2025. Downloaded on 6/6/2026 1:27:29 AM. This article is licensed under a Creative Commons Attribution-NonCommercial 3.0 Unported Licence.

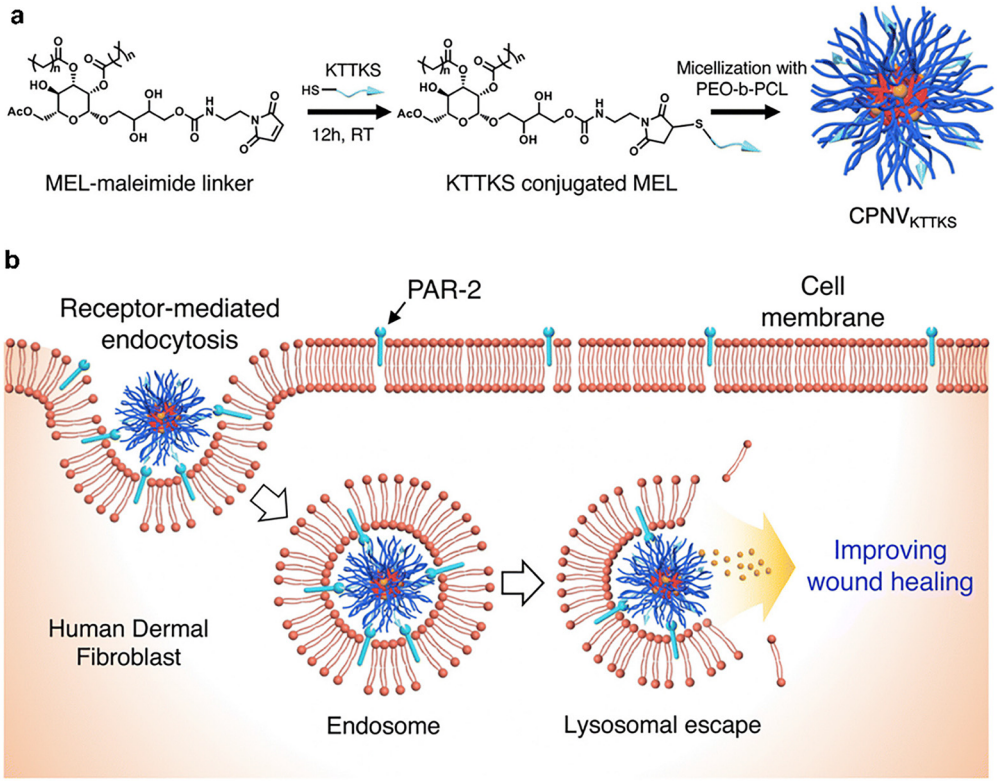

Fig. 7 (a) Peptide conjugation to the polymer *via* thiol–Michael addition and fabrication of micelle, and (b) schematic illustration of wound healing by targeted micelles through receptor-mediated endocytosis in a fibroblast cell. Reproduced with permission.[61] Copyright 2023, Royal Society of Chemistry.

predominantly on the membrane of fibroblasts, targeting peptide (KTTKS) was conjugated to MEL linker *via* thiol–maleimide reaction. The selectivity of the micelles towards the fibroblasts was confirmed *in vitro* by quantifying the internalized micelles co-cultured with three different skin cells. Targeted micelles were found to be internalized into fibroblasts 2-fold higher than other skin cells. Moreover, curcumin-loaded targeted micelles exhibit elevated collagen production and enhanced wound–healing abilities.

Besides the thiol-maleimide dyad, metal-free thiol–ene, thiol–yne, Schiff base, and SPAAC "click" chemistries were also investigated to arm micelles with targeting peptides. Diaz and coworkers employed the metal-free thiol–ene "click" chemistry for surface modification of micelle with GIRLRG peptide, which targets glucose-regulated protein GRP78 found in breast cancer.[188] Hao *et al.* grafted the Cys-Arg-Glu-Asp-Val-Trp peptide onto diallyl functionalized poly(ethylene glycol)-*b*-poly-(lactide-*co*-glycolide)-*g*-polyethylenimine (mPEG-*b*-PLGA-*g*-PEI-DA) *via* thiol–ene reaction.[189] This carrier targets endothelial cells suitable for rapid endothelialization of artificial blood vessels. Garg *et al.* synthesized a diblock copolymer where the side chain of the hydrophobic block owns an alkyne unit, which is further functionalized *via* an azide-containing fluorescent probe through a CuAAC reaction.[190] On the other hand, the breast cancer targeting peptide was installed on the aldehyde functionalized hydrophilic end of the diblock *via* a metal-free Schiff-base "click" reaction. The targeting efficiency was proven *in vivo*, where rapid tumor accumulation was observed for targeted micelles compared to their non-targeted counterparts. Ferrara and colleagues designed a unimicellar cancer nanovaccine for cancer immunotherapy.[191] The surface of the micelle was decorated with different melanoma peptide antigens through the SPAAC reaction. The end groups of the hyperbranched polymer were modified with DBCO units. Meanwhile, each peptide was azide functionalized along with the PEG mannose to introduce targeting peptides and aqueous soluble parts onto the hyperbranched polymer core *via* a metal-free SPAAC reaction. These nanovaccines have proven biocompatible, and *in vivo* application revealed tumor regression in B16 melanoma-bearing mice.

Among the several peptides employed for targeting, a small peptide Arg-Gly-Asp (RGD) stands out for its integrin receptor targeting property.[192,193] Integrins involve many biological pathways, such as wound healing, immune response, and angiogenesis. Although the RGD sequence was discovered in 1984, its targeting role in cancer was found in the early 2000s.[186] Since then, scientists have focused on its incorporation with drug delivery systems.[10,12,18,40,194–202] As for the conjugation of RGD peptide to micelles *via* "click" chemistry, an early example was reported in 2009 by Shoichet and colleagues.[53] They have designed a micellar drug delivery system with a modified RGD peptide for targeted delivery to

 This journal is © The Royal Society of Chemistry 2026

Open Access Article. Published on 24 November 2025. Downloaded on 6/6/2026 1:27:29 AM. This article is licensed under a Creative Commons Attribution-NonCommercial 3.0 Unported Licence.

the eye. Azide-terminated PEG-amine was coupled with poly(2-methyl-2-carboxytrimethylenecarbonate-*co*-D,L-lactide) (poly(TMCC-*co*-LA)) to obtain the diblock copolymer. Once the self-assembly occurs, azide groups are present on the surface of the micelle. An alkyne-modified RGD sequence containing peptide (KGRGDS) was installed on the surface of micelles *via* CuAAC ''click'' chemistry. In another study, Ke *et al*. linked hydrophilic and hydrophobic blocks with an RGD-bearing matrix metalloproteinase (MMP) responsive peptide sequence GPLGVRGDG *via* CuAAC ''click'' reaction.[203] When micelles reach the tumor site, overexpressed MMPs cleave the hydrophobic layer, exposing the RGD sequence, which leads to receptor-mediated endocytosis into tumor cells. The polymer side chain conjugation of cRGD by using CuAAC ''click'' reaction was recently reported by Ni and coworkers.[204] The polymer backbone was obtained from ROP of the 2-(but-3-yn-1-yolxy)-2-oxo-1,3,2-dioxaphospholane (BYP). Pendant alkyne groups were further functionalized with azide-bearing chemotherapy agent and cRGD-PEG-N_3 *via* CuAAC ''click'' reaction.

The need for mild reaction conditions and the ease of thiol functionality incorporation to the RGD peptide *via* the cysteine amino acid provides an opportunity to utilize thiol-based ''click'' reactions as an alternative way to conjugate RGD peptide to micelles. Many examples have been reported with the reaction of thiol–maleimide dyad as a metal-free ''click'' reaction.[62,205–208] Zhan *et al.* incorporate the thiol motif on the cRGDyK peptide first by reacting the amine end of lysine with 3,3′ dithiodipropionic acid and later by reducing it *via* DTT.[205] Thiol–Michael ''click'' reaction was performed between maleimide-terminated PEG–PLA and thiol-modified cRGDyK to obtain the targeted micelle. Kataoka and coworkers reported a cRGD conjugated polymeric micelle for the glioblastoma treatment.[206] Their system was composed of the mixture of poly(ethylene glycol)-*b*-poly(L-glutamic acid) (MeO-PEG-*b*-P(Glu)) and maleimide conjugated polymer Mal-PEG-*b*-P(Glu). Cysteine containing cRGD and cyclic-Arg-Ala-Asp (cRAD) peptides were linked to the PEG termini of the polymer *via* thiol–malemide ''click'' reaction to obtain targeted and non-targeted micelles, respectively. The varying ratio of the peptide-containing micelles was evaluated, and 20% cRGD-containing micelles could bypass the barriers and penetrate the tumor, whereas non-targeted micelles displayed limited tumor inhibitory effects.

Another elegant utilization of the thiol–maleimide ''click'' reaction for peptide and RGD conjugation was reported by Zheng and colleagues.[208] They developed a dual-targeted micelle for glioma treatment where the micelles were obtained *via* host–guest supramolecular interaction. To achieve this host–guest self-assembly, three different polymers were used which are Angiopep-2 conjugated polyethylene glycol(PEG)-β-cyclodextrin (Ang-2-PEG-βCD), cyclic RGD (cRGD)-PEG-βCD and fluorescein isothiocyanate (FITC) labeled adamantane-poly(ε-caprolactone) (Ad-PCL-FITC). Ang-2 mediates the blood-brain barrier penetration, where cRGD enhances the cellular uptake by tumor cells. DOX was used as a model drug, and FITC was used for tracking purposes. *In vitro* studies show the enhanced cellular internalization of dual-targeted micelles compared to free DOX and non-targeted micelles. A similar trend was observed in cytotoxicity studies. *In vivo* experiments further supported these findings and revealed better tumor inhibition was observed upon administering dual-targeted micelle. Recently, Huang *et al.* fabricated a cysteine-modified RGD conjugated to DSPE-PEG(2000)-maleimide *via* thiol–maleimide ''click'' reaction.[62] This time, they have used RGD to target autosomal dominant polycystic kidney disease rather than a cancer-targeting strategy. The integrin receptors are also found on the extracellular matrix of the basolateral surface of renal tubules, which is the exact location of the diseased site. With the encapsulation of four different drug candidates into the RGD-targeted micelles, they have shown the targeting ability to diseased sites and higher renal accumulation *in vivo*.

Even though thiol–maleimide was extensively studied, other metal-free ''click'' reactions like radical thiol–ene and SPAAC ''click'' reactions also gathered attention in RGD conjugation to micelles. Zhong and coworkers fabricated core crosslinked polypeptide micelles for DOX delivery to breast cancer.[210] cRGD targeted micelles obtained from the allyl terminated poly(ethylene glycol)-*b*-poly(L-tyrosine) (allyl-PEG-*b*-PTyr) *via* radical thiol–ene ''click'' reaction between the cRGD-SH and allyl terminus of block copolymer. This system was evaluated *in vitro*, and targeted micelles showed better cellular uptake and improved cytotoxicity profiles compared to non-targeted micelles and a clinical liposomal DOX formulation. Guo *et al.* synthesized a poly(ethylene oxide) (PEO)–poly(e-carprolactone) (PCL) diblock copolymer with a 4-dibenzocyclooctynol (DIBO) modified PEO terminus.[211] This DIBO residue was further functionalized with several azide-terminated targeting moieties like sugar, RGD, and biotin through a metal-free SPAAC ''click'' reaction. The cytotoxic effect of 7-ethyl camptothecin (7-Et-CPT) loaded RGD-targeted and non-targeted micelles was evaluated against the MCF-7 human breast cancer cell line.

In conclusion, peptide-based ligands offer enhanced binding capabilities and a range of diverse applications. They have been used in many constructs and have been attached using a variety of conjugation chemistries. Combination with micelles through ''click'' reaction has been widely investigated. Unlike sugars and vitamins, their conjugation with micelles through a metal-free ''click'' reaction has been employed in many examples. One can anticipate that as our understanding of disease mechanisms grows, new peptides for targeting purposes will continue to be developed, and would be installed on micellar surfaces to achieve better selectivity for disease cells.

2.6 Miscellaneous small molecule ligand based targeting

As discussed in the previous sections, most of the small molecule targeting ligands are either sugars, vitamins and peptides. In recent years, a few other small molecules have been evaluated as potential ligands, and their conjugation to micellar drug delivery systems using ''click'' chemistry has been reported.[212] For example, Chen *et al.* used diphosphoserine peptide and pyrophosphate as ligands against dental plaque formation.[213] They conjugated the diphosphoserine

Open Access Article. Published on 24 November 2025. Downloaded on 6/6/2026 1:27:29 AM. This article is licensed under a Creative Commons Attribution-NonCommercial 3.0 Unported Licence.

peptide *via* CuAAC "click" reaction to the hydrophilic ends of the Pluronic P123 polymer and fabricated antimicrobial agent encapsulated tooth-binding micelles. Liu and coworkers utilized a glucose transport protein 1 (GLUT1) targeted micelle where the dehydroascorbic acid (DHA) was used as the targeting ligand.[214] Their micelle system was composed of Paclitaxel (PTX) loaded poly L-phenylalanine (pPhe), 3,3′-dithiobis-(sulfosuccinimidyl propionate) (DTSSP) crosslinked poly L-lysine (pLys), polyethylene glycol (PEG), and dehydroascorbic acids (DHA) (DHA-PLys$_{(s\text{-}s)}$P/PTX). DHA was installed at the azide-modified PEG termini using the CuAAC "click" reaction. These micelles show an inhibitory effect on tumor cell viability, restraining tumor cell proliferation and migration *in vitro*. Additionally, *in vivo* studies support these results, displaying tumor regression and prolonged lifespan in tumor-bearing mice.

Combination therapies such as chemotherapy and photodynamic therapy can be employed to enhance the therapeutic outcome. Such an approach was reported by Gao *et al.*[215] They have investigated the epidermal growth factor receptor (EGFR) ligand, erlotinib, against non-small cell lung cancer (NSCLC). Chitosan was modified with an azide to utilize it for the CuAAC "click" reaction with alkyne-bearing erlotinib and NIR probe Cy7. The targeting efficiency of erlotinib was shown in cellular internalization, where the cells were chosen according to the ligand sensitivity. The ligand-sensitive cells displayed higher internalization compared to the ligand-resistant ones.

Leveraging the diseased sites' physiological conditions has been commonly employed for targeting strategies. The low pH of the tumor area has been extensively exploited in the fabrication of drug delivery systems by incorporating pH-responsive linkers or polymers into the carrier system. Besides using the acid-labile linkers, incorporating chargeable functional groups is another alternative. Nyström and colleagues adopted such an approach.[216] They choose histamine as a mitochondrion targeting group due to its charge reversibility in response to pH change. Poly(allyl glycidyl ether)-*b*-poly(ethylene oxide) (PAGE-*b*-PEO) block polymers was functionalized with histamine *via* UV-initiated thiol–ene "click" chemistry. DOX-loaded micelles obtained from 50% histamine-modified polymer showed higher internalization than the others. Luo and coworkers recently reported antibiotic-based micelles for bone targeting, where they employed vinylphosphonic acid for bone binding and conjugated it to the micelle surface through a thiol–ene "click" reaction.[217] These micelles were evaluated in an osteomyelitis model infected with MRSA, where they promoted bone healing.

Recently, phenylboronic acid (PBA) ligands have been utilized due to their ability to target the boronic acid transporters, and pH-dependent structural changes that enable this unit to function as both an active targeting ligand and a stimulus-responsive unit.[218,219] Numata and coworkers reported a phenylboronic acid-functionalized micelles for siRNA delivery to brown algae.[220] PBA bearing cell penetrating peptide sequence that contains a cysteine residue as a thiol group was conjugated to maleimide functionalized cationic peptide sequence through the thiol–maleimide "click" reaction for gene silencing.

Due to fast reaction kinetics, the SPAAC reaction has been used for the installation of ligand on micelle surfaces. Alsaab *et al.* designed a targeted micelle against renal cell carcinoma (RCC) by taking advantage of the overexpression of a tumor-hypoxic environment marker named carbonic anhydrase IX (CA IX).[221] Acetazolamide was used as a targeting ligand, and it was conjugated to the azide-terminated PEG side chains of the polymer through the SPAAC "click" reaction. Uptake in tumor spheroids demonstrated that targeted micelles penetrate more to the tumor core. Similarly, targeted micelles were internalized more than the non-targeted ones into the drug-resistant human RCC cells.

Although small molecule ligands can circumvent many biological barriers and penetrate more into tissues, the need for ligands having longer serum life, higher binding affinity, and selectivity continues. Many of the ligands discussed in this section suffer from either short half-life or accumulate below the expected rate in target sites due to the existence of their receptors along the body. In this regard, large targeting groups such as monoclonal antibodies and antibody fragments offer attractive solutions to address these challenges.

3. Monoclonal antibody based targeting

The invention of monoclonal antibodies (mAbs) by Kohler and Milstein was made from mouse hybridoma in 1975.[222] Along with the developments in biotechnology, chimeric antibodies, and humanized mAbs were developed.[223–225] These inventions garnered a steeping interest in mAbs due to the appealing advantages such as increased half-life in the serum and the excellent binding ability to their specific antigens.[226] Upon the FDA approval of mAbs, research on mAbs and their conjugates with small molecules like drugs and imaging agents intensified.[227–232] Conjugates of mAbs with polymers, dendrimers, hydrogels, nanogels, nanoparticles, and micelles have been extensively explored.[73,233–241] A wide range of chemistry has been utilized to install mAbs onto polymeric materials, many based on "click" chemistry transformations.[7,242–246] Within the scope of this review, we underscore the examples of immunomicelles, micelles chemically conjugated with mAbs at their surface, through "click" chemistry.[48,63,247–249,251–254,260–262]

Since the classification of DA as a "click" reaction, there has been a growing interest in utilizing DA with different polymeric materials, including micelles.[250] An early example was reported by Shoichet and coworkers, where furan functionalized outer PEG corona was coupled with maleimide containing anti-HER-2 antibody *via* the DA "click" reaction.[48] Each antibody was subjected to site-specific modification at the Fab side without compromising the binding efficiency of mab with two maleimide units. Antibody conjugation at the micelles' surface could be tuned by the reaction time and maleimide to furan feed ratio. Since the DA reaction can be performed under mild

 This journal is © The Royal Society of Chemistry 2026

Open Access Article. Published on 24 November 2025. Downloaded on 6/6/2026 1:27:29 AM.
This article is licensed under a Creative Commons Attribution-NonCommercial 3.0 Unported Licence.

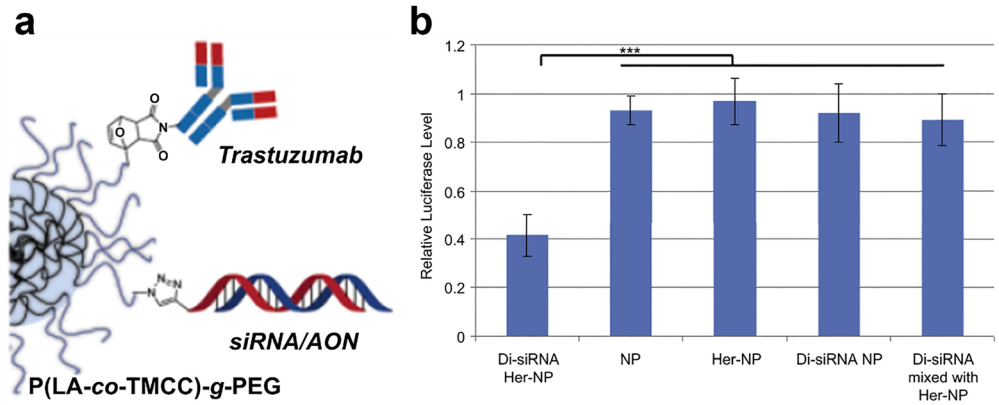

Fig. 8 (a) Dual functionalized micelles allowed antibody attachment through Diels Alder cycloaddition and oligonucleotide attachment *via* a CuAAC reaction. (b) Targeting effects and gene silencing efficiency of Her-NPs against HER2+ SKOV3-luc cells. Reproduced with permission.[251] Copyright 2013, Elsevier.

conditions in aqueous environment, it prevents the loss of antibody binding efficiency and its selectivity. Moreover, 1–2% of furan units were conjugated to antibodies, and the remaining furan units were available for further functionalization, such as drug or imaging agent conjugation. As an extension of this work, the authors reported the fabrication of dual-functionalized micelle by using both DA and CuACC "click" reactions to conjugate Trastuzumab and oligonucleotide, respectively.[251] The polymer was composed of poly(D,L-lactide-*co*-2-methyl-2-carboxytrimethylene carbonate)-*graft*-poly(ethylene glycol) (P(LA-*co*-TMCC)-*g*-PEG-furan/azide) and obtained micelles were coupled with Trastuzumab–maleimide using the DA "click" reaction and alkyne-functionalized oligonucleotides (ONs) with CuAAC "click" reaction to the PEG end groups for targeted gene silicing therapy (Fig. 8). This approach enables control over the amount of targeting antibody and oligonucleotide on the micelle surface.

However, a safety issue regarding biomedical applications might stem from using copper metal. To address this issue, the authors reported another work where the surface of the dual-functionalized micelles was decorated simultaneously with both furan and azide groups.[252] Dual-functionalized amphiphilic copolymer was composed of poly(D,L-lactide-*co*-2-methyl-2-carboxytrimethylene carbonate)-*graft*-poly(ethylene glycol) (P(LA-*co*-TMCC)-*g*-PEG-furan/azide). The micelle obtained from this polymer was sequentially coupled with Trastuzumab maleimide *via* DA "click" reaction and dibenzyl cyclooctyne (DBCO)-functionalized FLAG peptide through metal-free strain-promoted alkyne–azide cycloaddition (SPAAC) "click" reaction to the PEG end groups for theranostic applications. Both "click" reactions were suitable for aqueous reaction conditions and avoided metal-based toxicity.

Even though DA chemistry has appealing advantages like readily available reactants, requiring no catalyst or initiator, no toxic byproducts, and proceeding in an aqueous environment, the reaction requires a long time. In this regard, the SPAAC "click" reaction is an attractive alternative since it proceeds with faster kinetics. Hawker and colleagues evaluated the potential of the SPAAC "click" reaction to fabricate lipid nanoparticles armed with mAbs.[253] The authors employed a lipid-PEG micellar system where they could control the exact number of ethylene glycol units. The bromo end group was replaced with the azide functional group. Later, they used these polymers for fabricating a lipid nanoparticle system and conjugated the DBCO-modified antibody through the SPAAC reaction (Fig. 9). The work displays a convincing example for the fabrication of antibody-conjugated micellar nanoparticles using the SPAAC "click" reaction.

Zhong and coworkers reported a direct example of mAb conjugation to a micelle *via* SPAAC "click" reaction.[63] They designed a polypeptide micelle system where they have conjugated DBCO-modified Daratumumab, a CD38-targeted antibody, to the azide-functionalized micelle surface using the SPAAC reaction. The antibody per micelle ratio was chosen to be 3.2, and was obtained with 82% efficiency. The mAb appended micelle displayed a higher cellular internalization through endocytosis than its non-targeted counterpart. Moreover, this targeted delivery system exhibits a 6-fold higher inhibitory effect on CD38-positive multiple myeloma cells and also shows improved tumor growth inhibition and extended median survival time during *in vivo* studies.

Similar to the SPAAC "click" reaction, the inverse electron demand Diels–Alder (IEDDA) "click" reaction has garnered increased attention due to its exemplary features like fast reaction kinetics, catalyst-free conditions, high yield, benign side product (N_2 gas), selectivity, bioorthogonality, and biocompatibility.[6] These properties make this reaction an excellent choice for biomedical applications. Considering these appealing features, Zentel and colleagues utilized the IEDDA "click" reaction for *trans*-cyclooctene (TCO) bearing antibody conjugation ligation with 1,2,4,5-tetrazine functionalized polymeric micelles.[254] This intriguing work also investigates the ligation sites by comparing the micelles obtained from polymers that differ in the position and number of Tz groups, either bearing only one Tz at the hydrophilic end group or randomly distributed along the side chain (Fig. 10). Kinetic studies revealed that the second-order reaction rate was unaffected by

Open Access Article. Published on 24 November 2025. Downloaded on 6/6/2026 1:27:29 AM.
This article is licensed under a Creative Commons Attribution-NonCommercial 3.0 Unported Licence.

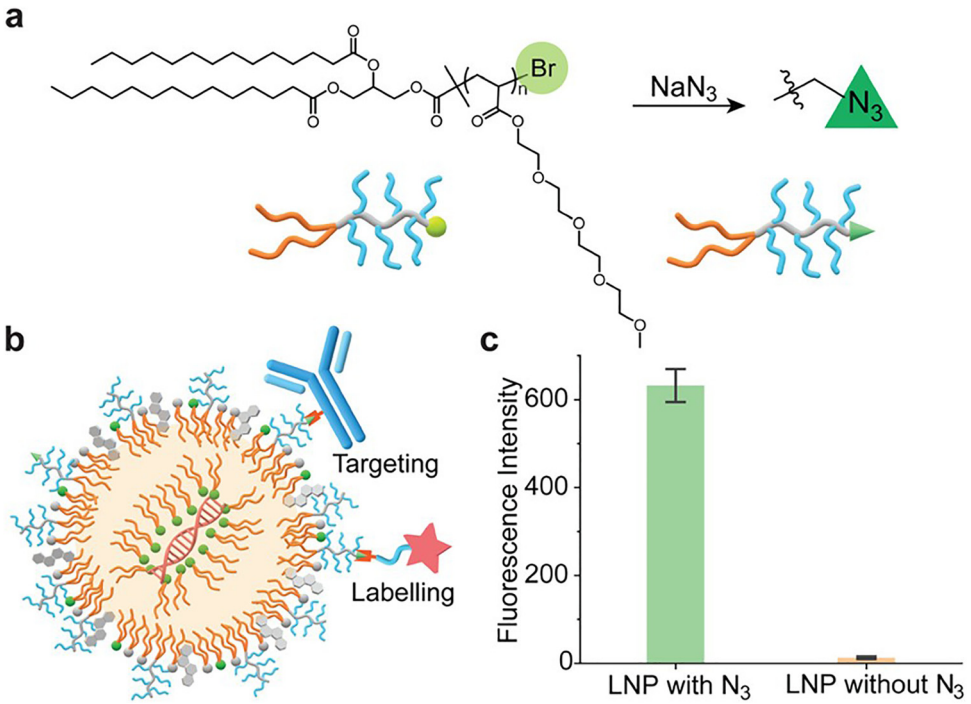

Fig. 9 (a) Preparation of the azido-ended oligomers. (b) Schematic illustration of lipid nanoparticles (LNPs) fluorophore labeling and antibody-directed targeting through "click" chemistry. (c) Fluorescence intensity of labeled LNPs. Reproduced with permission.[253] Copyright 2022, American Chemical Society.

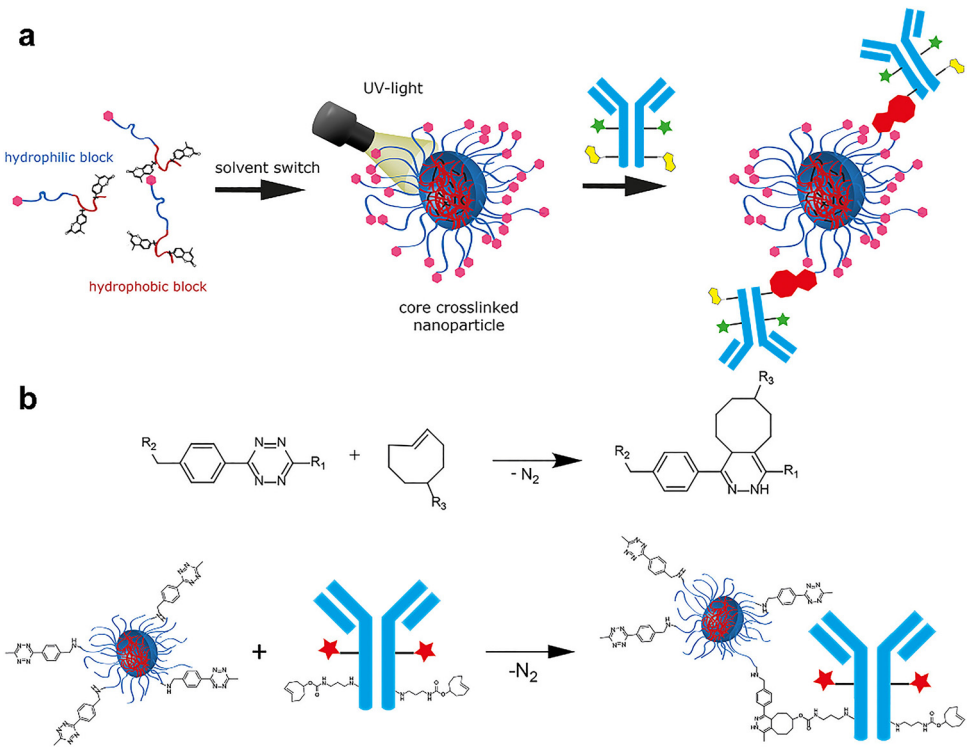

Fig. 10 (a) Schematic illustration of particle preparation followed by crosslinking to prepare the core-cross-linked micelles and the subsequent antibody "click" reaction. (b) Inverse electron demand Diels–Alder-initiated ligation between 1,2,4,5-tetrazines and trans-cyclooctenes. Reproduced with permission.[254] Copyright 2019, American Chemical Society.

 This journal is © The Royal Society of Chemistry 2026

Open Access Article. Published on 24 November 2025. Downloaded on 6/6/2026 1:27:29 AM. This article is licensed under a Creative Commons Attribution-NonCommercial 3.0 Unported Licence.

the conjugation of Tz to a macromolecule, and the increased number of Tz on the polymer chain increases the reactivity towards TCO groups on the antibody.

The high reactivity of the thiol group toward electron deficient alkenes has raised keen interest in conjugating biomacromolecules like mAbs or their derivatives onto various drug delivery systems, including micellar nanoparticles, since the reaction can be performed under mild conditions and in the absence of metal catalysts.[255–259] Depending on the nature of the alkene, thiol–Michael addition can be performed with a high yield. The maleimide moiety has been extensively studied for the thiol–Michael addition reaction among the various reactive alkenes. The thiol–maleimide "click" reaction was explored for the conjugation of Cetixumab onto micelle by Shih *et al.* in 2017.[260] They obtained micelles from a mixture of diblock copolymers, namely mPEG-poly(ε-caprolactone) (mPEG-PCL), maleimide-terminated poly(ethylene glycol)-PCL (Mal-PEG-PCL) and DTPA-PEG-*b*-PCL (NH_2-PEG-*b*-PCL). Near-infrared dye IR-780 was encapsulated into micelles, and maleimide units on the surface were clicked with thiol-functionalized Cetixumab after micelle formation. This system was evaluated against cells with low and high epidermal growth factor (EGFR) expression. As expected, high expression of EGFR cells showed better cellular uptake of Cetixumab conjugated micelles, and the targeted micelles exhibited better tumor accumulation *in vivo*.

A unique example was recently presented by Li *et al.*, who developed a stimuli-responsive core crosslinked micellar system where the crosslinker is modified from the curcumin and is suitable for azide–alkyne "click" reaction.[261] Moreover, they decorated the micelle surface with allyl groups ready for a radical thiol–ene "click" reaction with thiol-containing antibodies (Fig. 11). Different antibody grafting ratios were obtained, and the system with 82% grafting was chosen for further studies. These CD326-targeted micelles (R-mAb-CD326@CCL NPs) could actively target breast cancer cells and displayed enhanced therapeutic efficacy in animal models where the tumor was considerably suppressed. Using the drug derivative as a stimuli-responsive crosslinker and actively targeting the tumor side increases the bioavailability of the drug. Another utilization of the metal-free "click" reaction for antibody conjugation to micelles was reported by Peng *et al.*[262] PTX encapsulated worm-like micelles were obtained from the self-assembly of amphiphilic PCL2000-MPEG2000 and PCL5000-PEG2000-CHO polymers. An anti-HER-2 antibody, Herceptin™, was conjugated onto these micelles through an amine–aldehyde Schiff-Base "click" reaction. The obtained targeted carrier system was evaluated both *in vitro* and *in vivo*, showing better internalization, accumulation, and therapeutic effects.

Since the invention of monoclonal antibodies (mAbs), numerous applications have been developed, several involving their conjugation to micelles. Their delicate nature requires mild reaction conditions to prevent loss of binding ability. To this end, various reactions have been investigated. The earliest examples demonstrate the effective application of Diels–Alder and CuAAC "click" reactions with high efficiency. After the

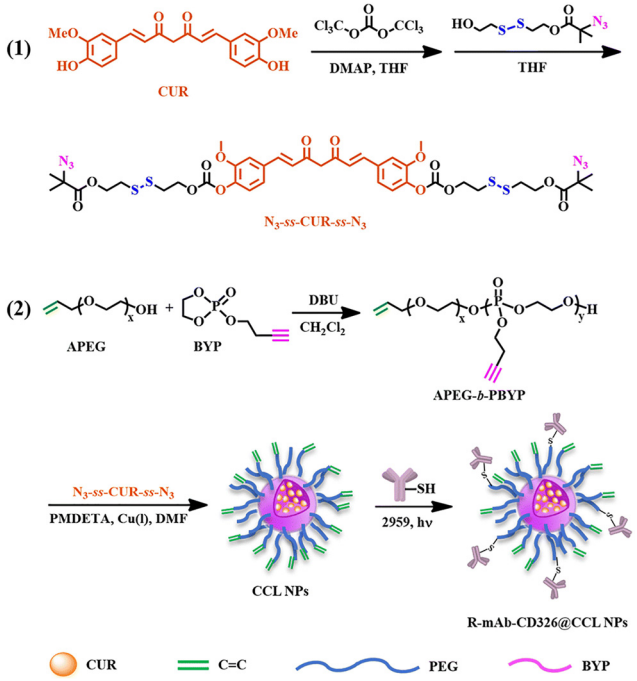

Fig. 11 Synthetic routes to core cross-linked nanoparticles modified by the CD326 monoclonal antibody. Reproduced with permission.[261] Copyright 2023, Royal Society of Chemistry.

classification of metal-free "click" reactions, this trend paves the way for the use of mAb conjugation onto micelles as well, due to mild and effective reaction kinetics. To this end, SPAAC, IEDDA, thiol–ene, and thiol–maleimide reactions have been employed for this purpose. Nevertheless, there is still room for further investigation, considering the limited examples of mAb-targeted micelles using "click" reactions as a conjugation strategy.

4. Antibody fragment-based targeting

Along with the investigation of mAbs, their smaller counterparts, fragments of antibodies (Fabs), are gaining attention due to some of their appealing features over mAbs. The whole antibodies have a larger size than Fabs, which makes them harder to penetrate solid tumors, even though they have extraordinary targeting ability to their corresponding receptors.[263,264] These improvements could be counterbalanced with a decreased half-life.[265,266] Increasing molecular weight by Fab conjugation to other structures was proposed as a solution, initially starting with pegylation.[267] Promising results from the pegylation trials led to the investigation of polymer–Fab conjugates.[268–271] Since then, several reports have emerged about conjugates of Fabs, such as, liposomes, polymer complexes, and micelles.[272–274] Incorporating Fabs onto polymeric scaffolds can be achieved using a variety of conjugation chemistries. Over the years a range of "click" reactions have bee employed for conjugating Fabs with nanomaterials, polymeric nanoparticles, liposomes, nanogels, and micelles.[245,258,275–280]

Open Access Article. Published on 24 November 2025. Downloaded on 6/6/2026 1:27:29 AM. This article is licensed under a Creative Commons Attribution-NonCommercial 3.0 Unported Licence.

In this section of the article, we showcase examples of Fab-conjugated micelles fabricated through "click" chemistry.

As an early report, Kataoka and coworkers developed an antibody-based therapeutic carrier against pancreatic tumors, where platinum-based drug-loaded polymeric micelles were conjugated with antibody fragments using the thiol–maleimide "click" reaction.[281] Each micelle was conjugated with one tissue factor (TF) targeting Fab' by tailoring the surface density of maleimide units. The targeted drug-loaded micelles displayed superior cellular binding than the non-targeted ones. Similarly, *in vitro* cytotoxicity profiles of targeted micelles were superior. *In vivo* tumor studies revealed higher tumor suppression upon treatment with targeted micelles, compared to treatment with non-targeted micelles and free drugs. In a recent study, Ji *et al.* described a targeted micelle system for delivering two synergistic siRNAs against pulmonary fibrosis (PF).[282] A cationic polymer, polyethyleneimine (PEI), grafted with maleimide-PEG (PEI-*g*-PEG-Mal) was utilized to obtain micelles upon complexation with siRNA. Targeting of lung-resident mesenchymal stem cells (LR-MSCs) was achieved by incorporation of anti-stem-cell antigen-1 antibody fragment (Fab') through a thiol–Michael "click" reaction (Fig. 12(a)). The inhibition of myofibroblast differentiation in the LR-MSCs was observed and tracked with the immunofluorescence images of Fab'-conjugated dual and single siRNA-loaded (Fig. 12(b)). The most significant decrease in the differentiated myofibroblasts was for Fab'-conjugated dual siRNA-loaded micelles. In another work, the authors used the same carrier system with varying maleimide ratios.[283] This time, Fab' fragment of the anti-platelet-derived growth factor receptor-α (PDGFRα) antibody was conjugated to the micelle surface using the thiol–maleimide "click" reaction for the co-delivery of two different siRNAs against the treatment of idiopathic pulmonary fibrosis. These examples showcase that the Fab targeting strategy can be diversified for specific antigen-displaying diseases other than several cancer types.

Christie and coworkers demonstrated the incorporation of Fabs onto micelles using the SPAAC "click" reaction in a proof-of-concept study to evaluate the conjugation and targeting efficiency of Fab-based targeted micelles.[284] They utilized a core crosslinked polyion complex micelle obtained from azide-functionalized PEG-*b*-poly(L-lysine) (N3-PEG-*b*-PLL) and azido-PEG-*b*-poly(aspartic acid) (N3-PEG-*b*-Pasp). Ephrin type-A receptor 2 (EphA2 receptor) binding fabs were engineered for site-specific conjugation through cysteine residues. For DBCO functionalization of Fabs, a heterobifunctional linker was reacted with the cysteine residues on Fabs *via* thiol maleimide reaction. Obtained Fab-DBCO was further reacted with azide displaying micelles through SPAAC "click" reaction, resulting in the conjugation of 2–3 Fabs per micelle. The cellular uptake of these micelles was shown to be higher than the mAbs, Fabs, and non-targeted micelles. In 2017, the same group optimized controlled Fab installation as a follow-up work by changing the Fab/polymer feed ratio and the spacer length between the Fab and micelle.[285] Moreover, they encapsulated a chemotherapy agent, SN38, into the micelles and evaluated these targeted micelles' internalization and cytotoxicity profiles.

To investigate the impact of Fab density on the micelle surface, Kataoka and colleagues developed Fab'-conjugated polyion complex (PIC) micelles for the delivery of small

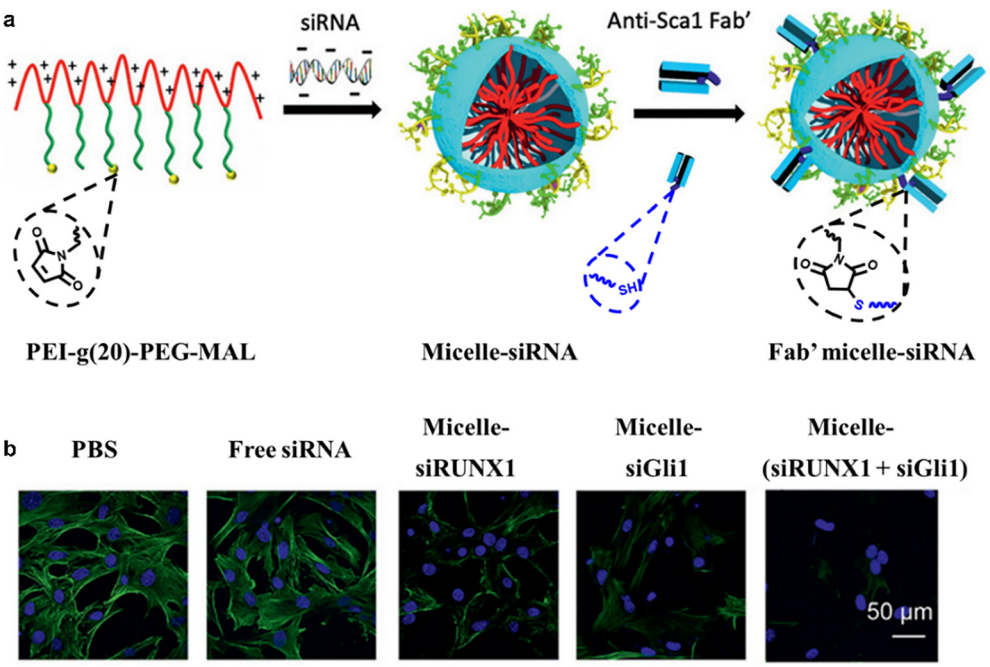

Fig. 12 (a) Formation scheme of siRNA-loaded micelle *via* the assembly and conjugation of Fab' to micelle surface *via* thiol–Michael addition for the targeting of lung mesenchymal stem cell, (b) actin expressions upon treatment with targeted micelle and control groups. Reproduced with permission.[282] Copyright 2021, Wiley.

 This journal is © The Royal Society of Chemistry 2026

Open Access Article. Published on 24 November 2025. Downloaded on 6/6/2026 1:27:29 AM.
This article is licensed under a Creative Commons Attribution-NonCommercial 3.0 Unported Licence.

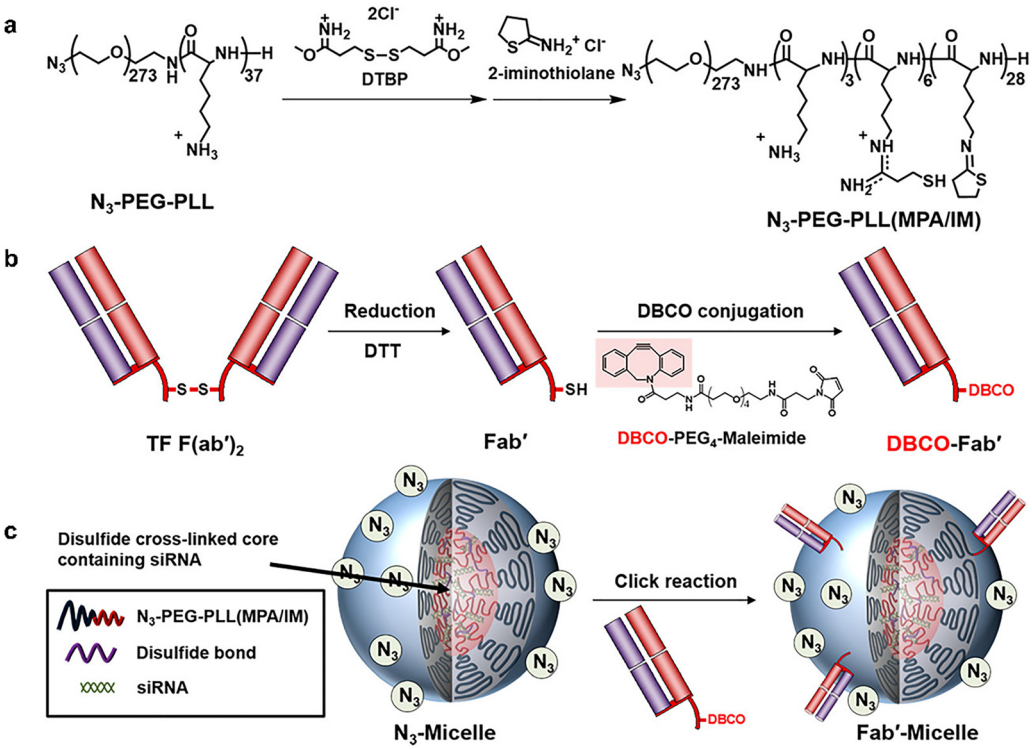

Fig. 13 Schematic illustration of Fab'-micelle construction. (a) The synthesis scheme of azide-functionalized block catiomer. (b) Preparation scheme of DBCO-Fab'. (c) DBCO-Fab' installation to N3-micelle. Reproduced with permission.[286] Copyright 2018, American Chemical Society.

interfering RNA (siRNA) to pancreatic cancer cells.[286] Azide-containing PIC micelles (N3 – Micelles) were obtained using a block copolymer of azide-functionalized poly(ethylene glycol)-*block*-poly(L-lysine modified with mercaptopropyl amidine and 2-iminothiolane) (N3-PEG-PLL(MPA/IM)) (Fig. 13). Core cross-linking of the micelles through disulfide bridges was accomplished after the siRNA encapsulation. Next, DBCO-modified antihuman tissue factor (TF) Fab' was conjugated onto the micelle surface using the SPAAC "click" reaction. By changing the feed ratio of Fab' to micelle (or azide), they were able to conjugate 1, 2, or 3 Fab'(s) per micelle. Cellular internalization analysis by flow cytometry and confocal laser scanning microscopy (CSLM) images revealed that 3(Fab')-micelles were more internalized in BxPC3 pancreatic cancer spheroid cells than the non-targeted counterparts. The most efficient gene silencing activity was observed with the 3(Fab')-micelle-treated cancer cells.

As another report, probing the effect of ligand density, Thurecht and coworkers reported a single-chain variable fragment (scFv) conjugated micellar system aimed to balance stealth behaviour and targeting both *in vitro* and *in vivo*.[64] Similar to the above examples, scFv conjugation was performed through a SPAAC reaction with a slight difference whereby DBCO was conjugated to micelles, and scFv was functionalized with azide. The results indicated that increasing the targeting ligand density does not always bring more advantages, and the optimum ratio for the ligand conjugation found *in vitro* may not yield the best outcome *in vivo*. Their *in vitro* results display the best outcome with 50% scFv density micelles, whereas the suitable option was 25% for *in vivo* application. The findings suggest that increasing the targeting ligand density in this case increases the immune response, which results in less tumor accumulation.

There is no doubt that antibody fragments offer several benefits over mAbs, yet these fragments also face challenges, such as short serum half-life. Conjugation with other structures may help to improve the serum life, but there might be some compromise with their binding affinity. Thus, although very promising, more work is needed to establish highly efficient approaches in the conjugation of mAbs to nanocarriers.

5. Oligonucleotide-based targeting

Oligonucleotides like DNA strands, RNA sequences, and aptamers are also widely employed for targeting purposes. Aptamers are recognition agents synthesized as short sequences of single-stranded nucleic acids DNA or RNA with unique intermolecular interactions that give rise to their specific three-dimensional conformation. They possess high affinity and specificity against target molecules like specific metal ions, small molecules, proteins, peptides, virus-infected cells, and cancer cells.[287–289] In 1990, Tuerk and Gold developed a process called "systematic evolution of ligand by exponential enrichment" (SELEX) to screen specific RNA species that are highly specific to their receptors.[290] In the same year, Ellington and Szostak also made contributions in this area and named these

Open Access Article. Published on 24 November 2025. Downloaded on 6/6/2026 1:27:29 AM. This article is licensed under a Creative Commons Attribution-NonCommercial 3.0 Unported Licence.

selected oligomers "aptamers."[291] There has been rapid progress in this area since then, and FDA approval of an aptamer drug named Macugen accelerated the research in aptamer technology.[292] The binding affinity of aptamers is very similar to that of mAbs; however, aptamers offer many superior properties compared to mAbs and antibody fragments. They have excellent stability in biological fluids and can quickly refold into their original structure and keep their activity due to their structural memory. They are resistant to denaturation and are stable against various environmental factors, like temperature. They have a smaller molecular weight and size than mAbs, which may enable deeper penetration into solid tumors. They lack the Fc region, which helps them evade immune cells, resulting in low immunogenicity.[158] With the various advantages of aptamers, investigations of aptamer-based applications are becoming widespread.[293–296] Aptamers have been utilized with various constructs, such as polymeric micelles, for applications in drug delivery. In this regard, the conjugation methods to the carriers have been investigated, including ones based on "click" chemistry.[297–300] Within the context of this review, in this section, we survey the work reported with oligonucleotide-conjugated micelles obtained using "click" chemistry.

An early example of single-stranded DNA (ssDNA) conjugation to a micelle was reported in 2011 by Maeda and colleagues.[58] They synthesized poly(*N*-isopropyl acrylamide) (PNIPAAm) polymer with an azide functional group at the chain end. Alkyne functionalized ssDNA was conjugated to PNIPAAm using the azide–alkyne "click" chemistry. This example represents the initial work for DNA conjugation to a micelle *via* "click" chemistry, but oligonucleotides were not used for targeting purposes.

Recent report focused on imaging and photodynamic therapy (PDT) applications of oligonucleotide micelles in tumor targeting was reported by Tian and colleagues, who designed a system for non-invasive imaging of glioblastoma uaing DNA nanotechnology.[301] The required diblock polymer was obtained *via* Huisgen-type CuAAC "click" reaction of polystyrene azide and DNA–alkyne, where DNA serves as both targeting and hydrophilic block of the micelle. NIR-II emitting dye was encapsulated for imaging purposes. *In vitro* traversing efficiency and internalization of Nile red loaded PS-*b*-DNA micelles and its PEG counterpart (PS-*b*-PEG) was evaluated. NR-loaded PS-*b*-DNA showed 4.5-fold higher traversing efficiency and a 3.0-fold increased accumulation in U87MG cells compared with NR@PS-*b*-PEG. Similarly, targeted micelles displayed better cellular uptake through receptor-mediated internalization.

Like many other ligand conjugation examples, metal-free "click" chemistry has been used for tethering of aptamers onto micelles. In this context, Sumerlin and coworkers reported an impressive work,[65] where they designed aptamer-conjugated micellar system for targeting colon cancer. A DBCO functionalized aptamer was attached to azide groups on the micelle surface through SPAAC "click" reaction after micelle formation (Fig. 14). This metal-free biorthogonal reaction also preserves the targeting function of aptamers. The authors produced 10%, 30%, and 100% azide-containing micelles and found that 10% azide-containing micelle results in less efficiency than 30% and 100% azide-functionalized micelles. Of the 30%

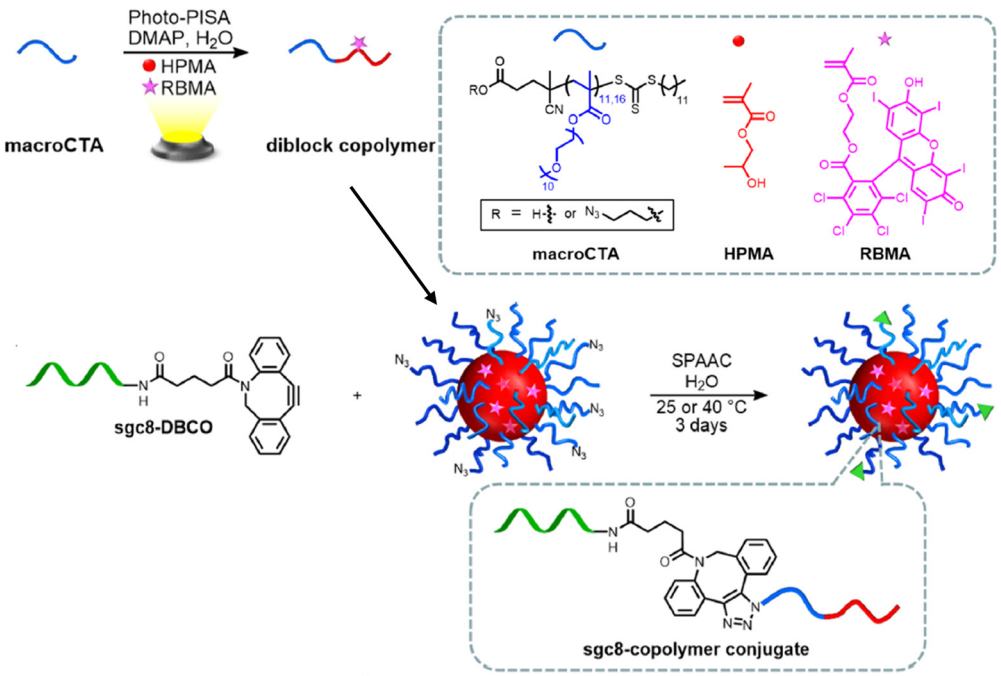

Fig. 14 Schematic representation of overall synthetic strategy to construct aptamer-modified nanoparticles. Azide-functionalized polymeric micelles are synthesized in one pot by self-catalyzed photo-PISA and modified by SPAAC with the sgc8-DBCO aptamer. Reproduced with permission.[65] Copyright 2020, American Chemical Society.

 This journal is © The Royal Society of Chemistry 2026

Open Access Article. Published on 24 November 2025. Downloaded on 6/6/2026 1:27:29 AM. This article is licensed under a Creative Commons Attribution-NonCommercial 3.0 Unported Licence.

azide-containing micelles, 14% of the groups were found to be conjugated to aptamer after purification. The Rose Bengal methacrylate (RMBA) monomer implemented in this work provides a fluorophore for imaging and acts as a singlet oxygen ($^1O_2$) generator for PDT.

Survey of reent literature indicate that oligonucleotides are emerging as promising ligands for targeting purposes, offering solutions to the challenges faced with employment of mAbs and Fabs. As for the conjugation strategy, the Huisgen-type CuAAC ''click'' reaction and metal-free ''click'' reactions, such as SPAAC, have been employed. Considering the limited examples of oligonucleotide-conjugated micelles, the area is open to further investigation and improvement.

6. *In vivo* ''click'' reaction-based targeting

Bioorthogonal chemistry continues to gain attention in therapeutic applications due to its engaging features, such as the realization of an efficient reaction in a mild physiological environment without affecting other biological processes, with high yield, fast kinetics, and selectivity.[302] The first bioorthogonal reaction using a modified Staudinger reaction was reported by Saxon and Bertozzi in 2000.[303] Since then, several other bioorthogonal ''click'' reactions have been reported.[41,304] The advancements in such reactions have increased the interest in employing bioorthogonal reactions in ''*in vivo*'' applications. This reaction has been investigated in metabolic glycoengineering applications as a two-component system. The approach entails anchoring different chemical functionalities onto biological surfaces such as cell membranes, through the inherent biological pathways. Administration of molecules/materials bearing their complementary reactive pair will trigger the reaction with previously labeled surfaces through bioorthogonal ''click'' chemistry in a highly selective manner.[302] The bioorthogonal metabolic glycoengineering tagging strategy has been investigated with various constructs over the years.[305–311] Micelles have been utilized in such systems, either as an anchoring compartment, or for both labeling and anchoring, as explained in systems highlighted below.[66,312–318]

In an elegant report, Xing and coworkers employed the *in situ* ''click'' targeting strategy for photoacoustic imaging-guided synergistic photothermal therapy (PTT) and photoacoustic therapy (PAT) using a single chromophore.[312] Zinc(II)–phthalocyanine (ZnPc) was encapsulated into an amino lipid–poly(ethylene glycol) (LP) DSPS-PEG2000-NH_2, and the surface of the micelle was further modified with DBCO (DBCO-ZnPc-LP). To begin with, tetraacetylated *N*-azidoacetyl-D-mannosamine (Ac_4ManNAz) encapsulated micelle was accumulated at the tumor site for the creation of the synthetic ''receptor-like'' azide groups through metabolic glycoengineering. Later, ZnPc loaded micelle was administered for conjugation at the tumor site through an *in vivo* bioorthogonal ''click'' reaction (Fig. 15). By uniting the synergy between PTT and PAT, potent therapeutic effects were seen both *in vivo* and *in vitro*.

Yang and colleagues reported another effective utilization of metabolic glycoengineering and bioorthogonal ''click'' targeting.[314] Using a similar approach to the abovementioned example, Ac_4ManNAz carrying micelles (Az-NPs) were used to introduce artificial receptors on the cell plasma membrane. Complementary reactive micelles (S-NP) were obtained using a

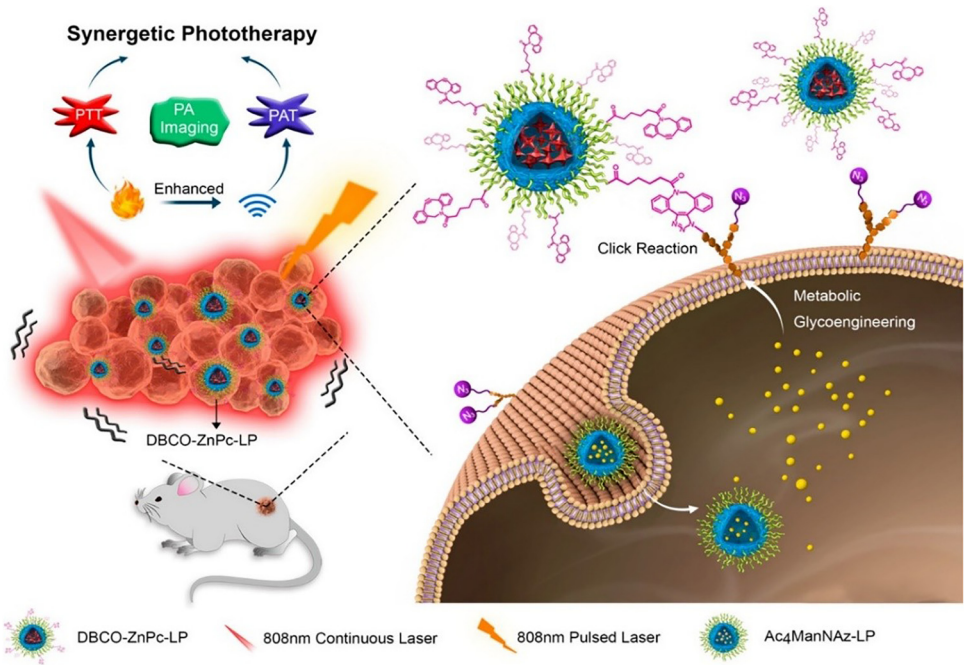

Fig. 15 Schematic illustration of bioorthogonal metabolic glycoengineering-activated tumor targeting micelle. Reproduced with permission.[312] Copyright 2017, American Chemical Society.

Open Access Article. Published on 24 November 2025. Downloaded on 6/6/2026 1:27:29 AM.
This article is licensed under a Creative Commons Attribution-NonCommercial 3.0 Unported Licence.

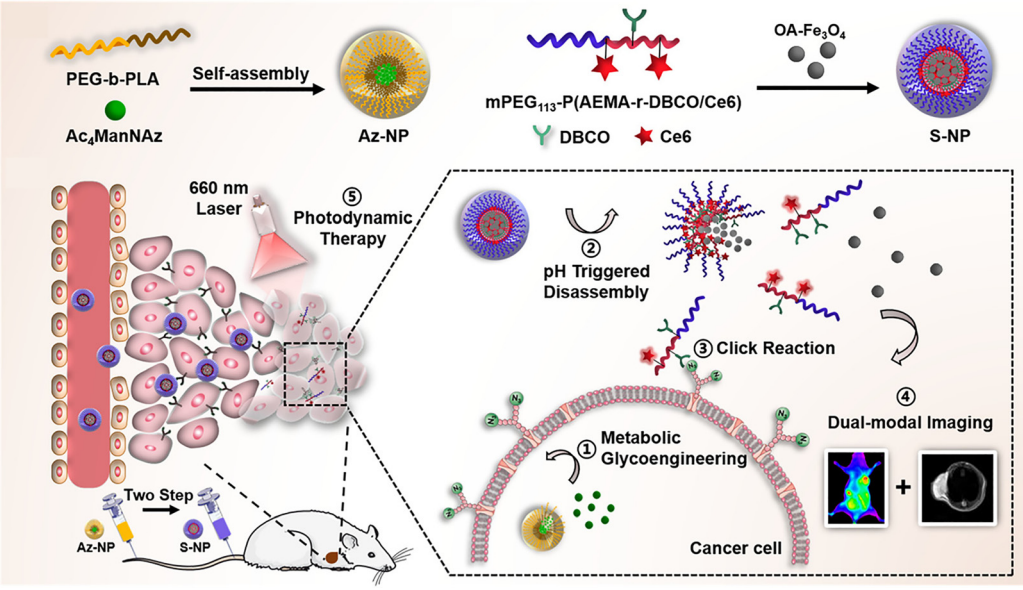

Fig. 16 Schematic illustration of a two-step acidity-activatable bioorthogonal pretargeting strategy. Reproduced with permission.[314] Copyright 2021, American Chemical Society.

polymer with pendant DBCO groups, a PDT agent chlorin e6 (Ce6), and acidic microenvironment-responsive units. Oleic acid-coated magnetic nanoparticles were encapsulated within this micelle to introduce MRI and theranostic attributes into the system. When S-NPs reach the tumor site, micelle disassembly occurs upon pH change, theus exposing the DBCO units and magnetic nanoparticles. DBCO and Ce6 bearing polymer chains undergo conjugation to the engineered tumor cells *via* the SPAAC reaction. Tumor cells anchored with Ce6 were exposed to laser irradiation for PDT, and enhanced cellular apoptosis was observed. Moreover, dual-modal tumor-specific visualization was achieved using T_2-weighted MR imaging (Fig. 16).

Li *et al.* developed a micellar system where one micelle is capable of inducing the azide-modified mannose expression on the tumor cell membrane; meanwhile, the other micelle housing ferroptosis agents can bind the tumor cell through *in vivo* bioorthogonal SPAAC chemistry due to the DBCO unit on the micelle surface.[315] This work also overcomes the lack of active targeting in ferroptosis since there are no targetable receptors for ferroptosis. The authors used a tumor-selective linker for the azide-modified mannose expression on the cell membrane. The micelles were obtained from polyethylene glycoldisulfide-*N*-azidoacetyl-D-mannosamine derivative where an 8-arm PEG-SS-COOH was conjugated on C6 position of the acetylated mannose azide (8ArmPEG-SS-AC3ManNAz). A similar strategy was applied for DBCO-modified micelles, where ferritinophagy initiator dihydroartemisinin (DHA) was conjugated to DBCO containing 8-arm PEG *via* a disulfide bond, and this micelle was also the host for ferroptosis inducer RSL3 (DBCO-8ArmPEG-SS-DHA@ RSL3). Azide was glycoengineered on tumor cells, and the ferroptosis was targeted through an *in vivo* metal-free "click" reaction by immobilizing the DBCO micelle on the tumor cells. The disulfide linker enhanced the therapeutic effect since the linker can be activated in tumor cells and release both cargos inside the cell. Yu and coworkers reported a similar metabolic glycoengineering approach for autoimmune disease treatment.[316] They used ROS-responsive nanoparticles as a carrier of azide-modified mannose (Ac4ManNAz) to the inflammatory tissue. Once azide groups are exposed to the cell membrane *via* metabolic glycoengineering, PD–L1 conjugated amphiphilic lipid (1,2-distearoyl-*sn-glycero*-3-phosphoethanolamine) (DSPE) functionalized with DBCO was administered for dual-anchoring immobilization of the protein on the cell membrane *via in situ* bioorthogonal metal-free SPAAC reaction, along with anchoring through physical interaction of the lipid tail with the cell membrane. Additionally, *in vivo* experiments showed that such an approach reversed early-onset type 1 diabetes (T1D) and delayed the development of rheumatoid arthritis (RA).

The bioorthogonal coupling highlighted in the abovementioned examples can also be executed through a different strategy. Instead of using the metabolic glycoengineering technique to anchor the second micellar compartment onto cell membranes, tumor microenvironment stimuli-induced aggregation might be an alternative approach. A micellar system can change conformation in the tumor environment and expose the multivalent DBCO or azide unit, allowing *in vivo* "click" reaction-induced aggregation at the tumor sites. Such an approach was reported by Deng *et al.*[317] The authors used a DBCO-functionalized PEG–PCL and PEG–imine–PCL polymer mixture to encapsulate DOX. An azide-functionalized PEG–PCL was employed for the second micelle encapsulating the transforming growth factor-β (TGF-β)/Smad3 signaling pathway inhibitor SIS3. Acid-labile imine bonds were cleaved in the tumor environment, exposing the azide and DBCO units to the

 This journal is © The Royal Society of Chemistry 2026

Open Access Article. Published on 24 November 2025. Downloaded on 6/6/2026 1:27:29 AM. This article is licensed under a Creative Commons Attribution-NonCommercial 3.0 Unported Licence.

surface of micelles. SPAAC "click" reaction-induced micelle aggregation, resulting in an increased tumor accumulation and reduced cellular efflux. A similar approach was employed by Yuan and coworkers to overcome hypoxic resistance and enhance chemoimmunotherapy.[318] Hidden DBCO groups were exposed on the micelle surface upon exposure to the decrease in the pH at the tumor site, which further reacted with the azide-functionalized micelles *via* SPAAC "click" reaction. The multivalency of these DBCO and azide groups leads to the formation of larger aggregates to increase the retention time in the tumor environment. To enhance the cellular uptake of these aggregates, the second acid-labeled functional group causes the slow dissociation of these aggregates into smaller particles. Encapsulated DOX and nitric oxide are delivered to the tumor cells, increasing the antitumor immune response while regulating hypoxia resistance.

Yu and colleagues presented a different approach for the *in vivo* "click" aggregation strategy.[66] They designed two different micellar systems, one containing DBCO and chargeable ethylene propyl amine groups on its side chains, namely mPEG-*b*-poly(ethylene propyl amine) (PED). The second micelle was composed of a mixture of three polymers, where one contains redox responsive disulfide bond linker bearing PROTAC (PROteolysis TArgeting Chimeras), the second one is an azide terminated version of the first one, and the third polymer contains a PDT agent. When the first injection containing PED micelles reaches the tumor side, protonation of the ethylene propyl amine groups due to the acidic pH of the tumor results in the disassembly of micelle and exposes the DBCO groups. Upon the arrival of azide-functionalized POLY-PROTAC micelles to the tumor site, micellar aggregation occurs due to the *in vivo* SPAAC "click" reaction between the DBCO groups of PED polymer chains and POLY-PROTAC micelles (Fig. 17). Rather than active targeting or anchoring the micelles onto tumor cells through *in vivo* "click," the authors promote passive targeting *via* "click"-induced micelle aggregation. This aggregation enhances the accumulation of therapeutic agents *in vivo*, and MDA-MB-231 tumour-bearing

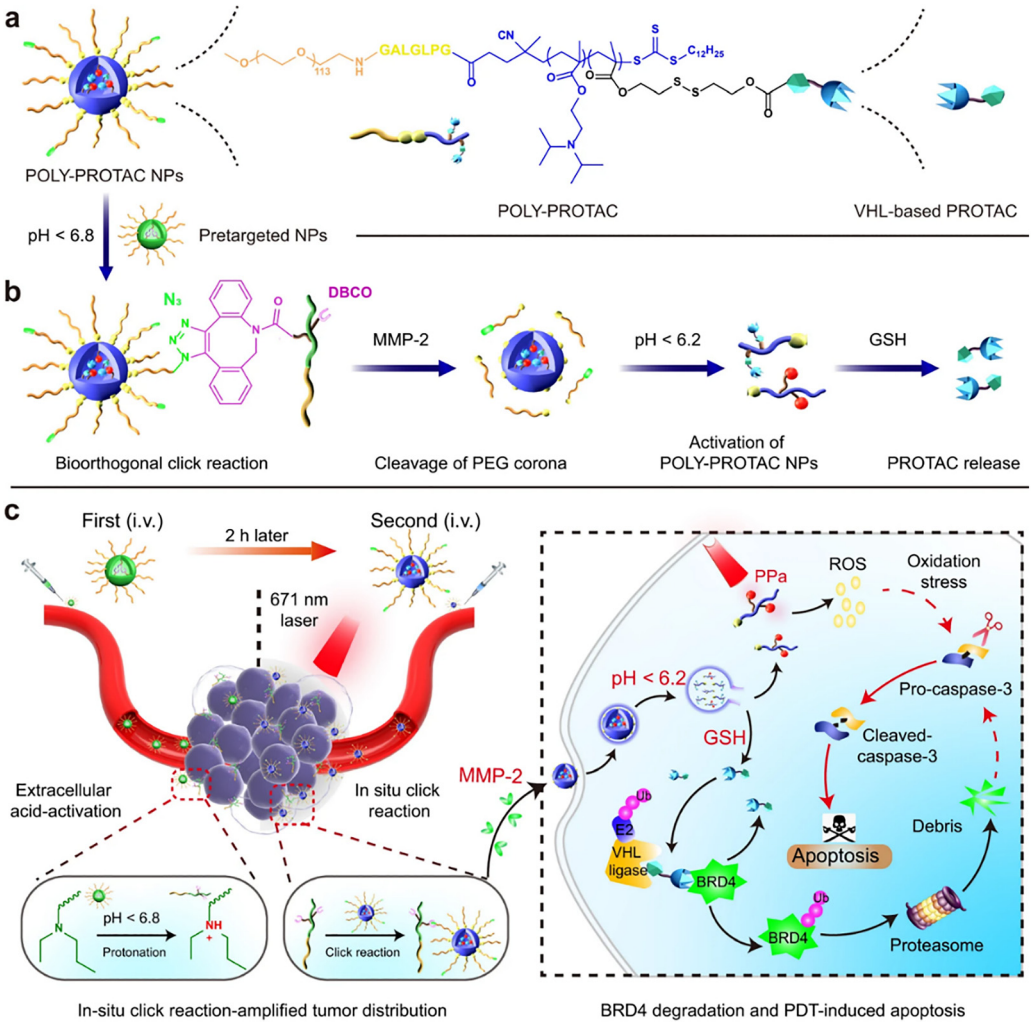

Fig. 17 (a) Cartoon illustration of the azide-functionalized bioorthogonal POLY-PROTAC NPs. (b) Schematic illustration of the extracellular acidity-triggered "click" reaction between POLY-PROTAC and DBCO-loaded pre-targeted NPs. (c) *In situ* "click" reaction-promoted protein degradation and combinatorial cancer therapy with POLY-PROTAC NPs. Reproduced with permission.[66] Copyright 2022, Springer Nature.

Open Access Article. Published on 24 November 2025. Downloaded on 6/6/2026 1:27:29 AM. This article is licensed under a Creative Commons Attribution-NonCommercial 3.0 Unported Licence.

nude mice treated with these nanoparticles displayed brighter intatumoral flouresence signal.

The bioorthogonal metabolic glycoengineering tagging strategy has gained attention in more recent years. Since this strategy employs an *in vivo* ''click'' reaction, it requires mild and fast reaction conditions. The metal-free SPAAC ''click'' reaction has been used in most examples to meet these criteria. Since such *in vivo* approaches are recent, one can expect to see many more examples in coming years.

7. Limitations and future perspective

Although targeted micelles have shown potential in various applications, several challenges must be overcome to translate them into clinical applications. The advantages of targeting ligands have been discussed throughout each section; however, there are also challenges associated with the use of ''click'' chemistry in drug delivery applications. The CuAAC ''click'' reaction is the most widely used ''click'' reaction since its early development. However, there has been a shift toward metal-free ''click'' reactions due to concerns about the toxicity stemming from the residual copper-based impurities. As an alternative to the CuAAC reaction, the Diels–Alder (DA) reaction was also widely employed as a metal-free ''click'' reaction for ligand conjugation. This reaction was invented by Otto Diels and Kurt Alder, who were also recipients of the Nobel Prize for this discovery in 1950.[319] The [4+2] cycloaddition reaction between an electron-deficient dienophile and an electron-rich diene is used for conjugations due to its several advantages, such as its selectivity and mild reaction conditions.[6,319] Although the DA reaction is mostly catalyst- and byproduct-free, the slow reaction kinetics and the possibility of having a mixture of endo and exo products limit its use in biomedical applications. To address this issue, Lewis acids can be used to accelerate the reaction rate; however, this approach may not be suitable for all ligands, especially those that are acid-sensitive.[6,320,321] Unreacted groups on the surface of micelles may be of concern, *e.g.* if there is unreacted maleimide after the DA reaction based ligand conjugation, biological substances, such as proteins (which often contain thiol functional group), may react with the residual maleimide groups, raising concern about uncontrolled interaction in biological environments.[6,320–322] Another metal-free ''click'' reaction is the strain-promoted azide–alkyne cycloaddition (SPAAC) reaction, which also provides bioorthogonality. Initially, this is an old cycloaddition reaction,[323] the reaction has gained more attention following the work of Bertozzi and colleagues, who reported the use of this reaction in living cells.[324] This reaction requires no catalyst and provides bioorthogonality without any byproducts. However, one of the limitations of SPAAC is the stability of these ring-strained cyclooctynes and the multistep synthesis requirement. As seen from the examples in this review, the IEDDA reaction is one of the most employed metal-free ''click'' reactions in biomedical applications. The reaction provides bioorthogonality, biocompatibility, fast reaction kinetics, catalyst-free reaction conditions, and proceeds with high selectivity. Due to these appealing features, this reaction has been widely employed for glycometabolic engineering, paving the way for *in vivo* ''click'' reactions. Nonetheless, this reaction also requires the use of strained alkynes, which often requires multistep synthesis, and tetrazine dienophile suffers from stability and requires a multistep synthesis.[6,325–329]

Among the nanosized drug delivery systems, targeted micelles stand out as a promising carrier for various biomedical applications as highlighted in this review. Although targeted micelles have been investigated for a long time, their clinical translation into healthcare applications is rather limited due to several factors and knowledge gaps in the area, such as efficient end-product analysis methods and optimization processes to prevent batch-to-batch variations, along with the quest to obtain the best outcome from that particular design. For bench-to-bedside translation, it is important to have an optimized synthesis procedure and achieve the same outcome from each batch. Future studies should focus on the optimal ligand density for the best outcome in case of a particular type of disease. Most of the time, ligand density on micelles has not been thoroughly investigated to determine the optimal ligand amount in terms of targeting efficiency and selectivity. Generally, the comparison between nontargeted and targeted micelles was presented, proving that the targeted ones display superior profiles compared to their nontargeted counterparts. In order to achieve optimization, better analytical techniques are needed to determine the surface ligand density and their orientation, as well as the homogeneity of the obtained micelles.

8. Conclusion

The examples highlighted in this review demonstrate that the development of ligand-targeted polymeric micelles is significantly accelerating research aimed at overcoming the limitations of conventional drug delivery. The innovations enabling this lie at the interface of polymer chemistry and bioorthogonal conjugation strategies. Central to this progress is the pivotal role played by ''click'' chemistry in transforming the way ligands are introduced onto nanocarriers. The high fidelity, selectivity, and mild reaction conditions of both copper-catalyzed and metal-free ''click'' transformations have enabled precise control over surface functionalization, which is critical for obtaining effective drug delivery systems. These highly modular chemistries aim to not only simplify the fabrication of complex micellar architectures but also allow for rapid screening and optimization of ligand presentation. Moreover, the emergence of *in vivo*-compatible ''click'' reactions, such as strain-promoted cycloadditions and tetrazine ligations, has further expanded the potential of ''click''-based systems. Looking ahead, the continued refinement of ''click'' transformations toward greater biocompatibility, tunability, and reaction speed will be instrumental in translating these materials from bench to bedside. However, challenges remain in scaling up the synthesis, while ensuring batch-to-batch consistency, and

 This journal is © The Royal Society of Chemistry 2026

Open Access Article. Published on 24 November 2025. Downloaded on 6/6/2026 1:27:29 AM. This article is licensed under a Creative Commons Attribution-NonCommercial 3.0 Unported Licence.

navigating the complex regulatory landscape before these could move to the market. Addressing issues such as micelle stability, ligand bioactivity retention, and immune compatibility will be key to eventual clinical success. Nonetheless, the synergy between advanced polymer design and efficient "click" chemistry based conjugation technologies provides a robust platform for engineering smart, multifunctional micelles. It is anticipated that the unique advantages of "click" chemistry will play a pivotal role in advancing the clinical translation of targeted nanomedicines from the lab to the clinic.

Author contributions

Enfal Civril: writing – original draft. Rana Sanyal: review & editing, supervision. Amitav Sanyal: conceptualization, writing, review & editing, supervision.

Conflicts of interest

There are no conflicts to declare.

Data availability

No primary research results, software or code have been included and no new data were generated or analysed as part of this review.

Notes and references

1 H. Ma, F. Xing, Y. Zhou, P. Yu, R. Luo, J. Xu, Z. Xiang, P. M. Rommens, X. Duan and U. Ritz, *J. Mater. Chem. B*, 2023, **11**, 7873–7912.
2 X.-Y. Zhou, C.-K. Wang, Z.-F. Shen, Y.-F. Wang, Y.-H. Li, Y.-N. Hu, P. Zhang and Q. Zhang, *J. Mater. Chem. B*, 2024, **12**, 7246–7266.
3 K. Liu, J. Xiang, G. Wang, H. Xu, Y. Piao, X. Liu, J. Tang, Y. Shen and Z. Zhou, *ACS Appl. Mater. Interfaces*, 2021, **13**, 44028–44040.
4 I. Altinbasak, Y. Alp, R. Sanyal and A. Sanyal, *Nanoscale*, 2024, **16**, 14033–14056.
5 S. Gulati, N. Ansari, Y. Moriya, K. Joshi, D. Prasad, G. Sajwan, S. Shukla, S. Kumar and R. S. Varma, *J. Mater. Chem. B*, 2024, **12**, 11887–11915.
6 A. Degirmenci, R. Sanyal and A. Sanyal, *Bioconjugate Chem.*, 2024, **35**, 433–452.
7 U. Huynh, P. Wu, J. Qiu, T. Prachyathipsakul, K. Singh, D. J. Jerry, J. Gao and S. Thayumanavan, *Biomacromolecules*, 2023, **24**, 849–857.
8 F. Calik, A. Degirmenci, R. Sanyal and A. Sanyal, *Eur. Polym. J.*, 2023, **201**, 112548.
9 P. Wu, J. Gao, P. Prasad, K. Dutta, P. Kanjilal and S. Thayumanavan, *Biomacromolecules*, 2022, **23**, 339–348.
10 A. Degirmenci, H. Ipek, R. Sanyal and A. Sanyal, *Eur. Polym. J.*, 2022, **181**, 11645.
11 Z. Jiang, S. Huo, L. Qiao, P. Lin, L. Fu, Y. Wu, W. Li, C. Bian, Y. Li, N. Li, H. Cheng, X. Nie and S. Ding, *J. Mater. Chem. B*, 2024, **12**, 8465–8476.
12 S. Kocak, B. Demirkol, R. Kilic Boz, R. Sanyal and A. Sanyal, *Polym. Chem.*, 2025, **16**, 1272–1284.
13 M. Dhara (Ganguly), *J. Macromol. Sci., Part A: Pure Appl. Chem.*, 2024, **61**, 265–288.
14 N. B. Basutkar, S. G. Surapaneni, S. Alam and A. V. Ambade, *J. Macromol. Sci., Part A: Pure Appl. Chem.*, 2024, **61**, 105–116.
15 E. Civril, A. Sanyal and R. Sanyal, *J. Macromol. Sci., Part A: Pure Appl. Chem.*, 2025, DOI: 10.1080/10601325.2025.2545324.
16 A. N. Lukyanov and V. P. Torchilin, *Adv. Drug Delivery Rev.*, 2004, **56**, 1273–1289.
17 Z. Ahmad, A. Shah, M. Siddiqa and H.-B. Kraatz, *RSC Adv.*, 2014, **4**, 17028–17038.
18 F. Calik, A. Degirmenci, M. Eceoglu, A. Sanyal and R. Sanyal, *Bioconjugate Chem.*, 2019, **30**, 1087–1097.
19 P. Jia, Y. Zou and J. Jiang, *J. Mater. Chem. B*, 2023, **11**, 11319–11334.
20 F. Chibhabha, Y. Yang, K. Ying, F. Jia, Q. Zhang, S. Ullah, Z. Liang, M. Xie and F. Li, *J. Mater. Chem. B*, 2020, **8**, 7438–7452.
21 K. Manna, A. Roy, S. Dey, S. Ghosh, P. Pradhan and S. Pal, *J. Macromol. Sci., Part A: Pure Appl. Chem.*, 2024, **61**, 349–375.
22 A. Mondal, S. Dey, S. Paul, A. Gupta and P. De, *Small*, 2025, **21**, 2502727.
23 S. R. Croy and G. S. Kwon, *Curr. Pharm. Des.*, 2006, **12**, 4669–4684.
24 S. C. Owen, D. P. Y. Chan and M. S. Shoichet, *Nano Today*, 2012, **7**, 53–65.
25 M. Talelli, M. Barz, C. J. F. Rijcken, F. Kiessling, W. E. Hennink and T. Lammers, *Nano Today*, 2015, **10**, 93–117.
26 L. Taiariol, C. Chaix, C. Farre and E. Moreau, *Chem. Rev.*, 2022, **122**, 340–384.
27 H. Maeda, *J. Controlled Release*, 2012, **164**, 138–144.
28 R. d'Arcy and N. Tirelli, *Polym. Adv. Technol.*, 2014, **25**, 478–498.
29 V. P. Torchilin, *Eur. J. Pharm. Sci.*, 2000, **11**, S81–S91.
30 Y. Zheng, Y. Oz, Y. Gu, N. Ahamad, K. Shariati, J. Chevalier, D. Kapur and N. Annabi, *Nano Today*, 2024, **55**, 102147.
31 M. S. Wadhwa and K. G. Rice, *J. Drug Targeting*, 1995, **3**, 111–127.
32 K. Jain, P. Kesharwani, U. Gupta and N. K. Jain, *Biomaterials*, 2012, **33**, 4166–4186.
33 A. Degirmenci, R. Sanyal and A. Sanyal, *RSC Appl. Polym.*, 2024, **2**, 976–995.
34 I. Altinbasak, M. Arslan, R. Sanyal and A. Sanyal, *Polym. Chem.*, 2020, **11**, 7603–7624.
35 E. J. Bolívar-Monsalve, M. M. Alvarez, S. Hosseini, M. A. Espinosa-Hernandez, C. F. Ceballos-González, M. Sanchez-Dominguez, S. R. Shin, B. Cecen, S. Hassan, E. D. Maio and G. T.-de Santiago, *Mater. Adv.*, 2021, **2**, 4447–4478.
36 M. Arslan, A. Degirmenci, R. Sanyal and A. Sanyal, *Polym. Chem.*, 2024, **15**, 4173–4195.

Open Access Article. Published on 24 November 2025. Downloaded on 6/6/2026 1:27:29 AM. This article is licensed under a Creative Commons Attribution-NonCommercial 3.0 Unported Licence.

37 B. Cengiz, N. Ejderyan and A. Sanyal, *J. Macromol. Sci., Part A: Pure Appl. Chem.*, 2022, **59**, 443–455.
38 H. Lin, H. Bai, Z. Yang, Q. Shen, M. Li, Y. Huang, F. Lv and S. Wang, *Chem. Commun.*, 2022, **58**, 7232–7244.
39 N. R. B. Boase, E. R. Gillies, R. Goh, R. E. Kieltyka, J. B. Matson, F. Meng, A. Sanyal and O. Sedláček, *Biomacromolecules*, 2024, **25**, 5417–5436.
40 M. A. Gauthier, M. I. Gibson and H. A. Klok, *Angew. Chem., Int. Ed.*, 2009, **48**, 48–58.
41 H. C. Kolb, M. G. Finn and K. B. Sharpless, *Angew. Chem., Int. Ed.*, 2001, **40**, 2004–2021.
42 R. Hoogenboom, *Chem*, 2023, **9**, 2416–2424.
43 K. Ghosal, S. K. Bhattacharyya, V. Mishra and H. Zuilhof, *Chem. Rev.*, 2024, **124**, 13216–13300.
44 U. S. Gunay, U. Tunca and H. Durmaz, *J. Macromol. Sci., Part A: Pure Appl. Chem.*, 2024, **61**, 143–154.
45 A. Khan, *Chem. Commun.*, 2023, **59**, 11028–11044.
46 E. Çakmakcı, *J. Macromol. Sci., Part A: Pure Appl. Chem.*, 2023, **60**, 817–840.
47 E. Lallana, F. Fernandez-Trillo, A. Sousa-Herves, R. Riguera and E. Fernandez-Megia, *Pharm. Res.*, 2012, **29**, 902–921.
48 M. Shi, J. H. Wosnick, K. Ho, A. Keating and M. S. Shoichet, *Angew. Chem., Int. Ed.*, 2007, **46**, 6126–6131.
49 P. De, S. R. Gondi and B. S. Sumerlin, *Biomacromolecules*, 2008, **9**, 1064–1070.
50 G. Chen, S. Amajjahea and M. H. Stenzel, *Chem. Commun.*, 2009, 1198–1200.
51 M. Prabaharan, J. J. Grailer, D. A. Steeber and S. Gong, *Macromol. Biosci.*, 2009, **9**, 744–753.
52 X. Wang, L. Liu, Y. Luo and H. Zhao, *Langmuir*, 2009, **25**, 744–750.
53 J. Lu, M. Shi and M. S. Shoichet, *Bioconjugate Chem.*, 2009, **20**, 87–94.
54 M. A. Azagarsamy, V. Yesilyurt and S. Thayumanavan, *J. Am. Chem. Soc.*, 2010, **132**, 4550–4551.
55 J. Kumar, L. McDowall, G. Chend and M. H. Stenzel, *Polym. Chem.*, 2011, **2**, 1879–1886.
56 X. Li, Y. Qian, T. Liu, X. Hu, G. Zhang, Y. You and S. Liu, *Biomaterials*, 2011, **32**, 6595–6605.
57 N. M. Barkey, N. K. Tafreshi, J. S. Josan, C. R. De Silva, K. N. Sill, V. J. Hruby, R. J. Gillies, D. L. Morse and J. Vagner, *J. Med. Chem.*, 2011, **54**, 8078–8084.
58 P. Pan, M. Fujita, W.-Y. Ooi, K. Sudesh, T. Takarada, A. Goto and M. Maeda, *Polymer*, 2011, **52**, 895–900.
59 J. K. Elter, S. Quader, J. Eichhorn, M. Gottschaldt, K. Kataoka and F. H. Schacher, *Biomacromolecules*, 2021, **22**, 1458–1471.
60 J. Olejniczak, G. Collet, V. A. N. Huu, M. Chan, S. Leea and A. Almutairi, *Biomater. Sci.*, 2017, **5**, 211–215.
61 Y. Lee, S. Kim, J. Seo, H. K. Kim, Y. P. Han, E. J. Park, J. O. Park, C.-S. Yang and J. W. Kim, *Biomater. Sci.*, 2023, **11**, 450–460.
62 Y. Huang, A. Osouli, J. Pham, V. Mancino, C. O'Grady, T. Khan, B. Chaudhuri, N. M. Pastor-Soler, K. R. Hallows and E. J. Chung, *Biomacromolecules*, 2024, **25**, 2749–2761.
63 R. Chen, J. Yang, Y. Mao, X. Zhao, R. Cheng, C. Deng and Z. Zhong, *Biomacromolecules*, 2023, **24**, 5371–5380.
64 A. J. Sivaram, A. Wardiana, S. Alcantara, S. E. Sonderegger, N. L. Fletcher, Z. H. Houston, C. B. Howard, S. M. Mahler, C. Alexander, S. J. Kent, C. A. Bell and K. J. Thurecht, *ACS Nano*, 2020, **14**, 13739–13753.
65 A. B. Korpusik, Y. Tan, J. B. Garrison, W. Tan and B. S. Sumerlin, *Macromolecules*, 2021, **54**, 7354–7363.
66 J. Gao, B. Hou, Q. Zhu, L. Yang, X. Jiang, Z. Zou, X. Li, T. Xu, M. Zheng, Y.-H. Chen, Z. Xu, H. Xu and H. Yu, *Nat. Commun.*, 2022, **13**, 4318.
67 D. Kapoor, S. Bhatt, M. Kumar, R. Maheshwari and R. K. Tekade, *Basic Fundamentals of Drug Delivery*, Academic Press, 2019, pp. 307–342.
68 L. Dai, J. Liu, Z. Luo, M. Lia and K. Cai, *J. Mater. Chem. B*, 2016, **4**, 6758–6772.
69 S. Muro, *J. Controlled Release*, 2012, **164**, 125–137.
70 J. Wang, T. T. Wang, P. F. Gaoa and C. Z. Huang, *J. Mater. Chem. B*, 2014, **2**, 8452–8465.
71 M. Yu, R. Cao, Z. Ma and M. Zhu, *J. Mater. Chem. B*, 2023, **11**, 1416–1433.
72 X. Jiang, Y. Zhao, S. Sun, Y. Xiang, J. Yan, J. Wang and R. Pei, *J. Mater. Chem. B*, 2023, **11**, 6172–6200.
73 B. S. Bolu, B. Golba, R. Sanyal and A. Sanyal, *Biomater. Sci.*, 2020, **8**, 2600–2610.
74 H. Freichels, R. Jérôme and C. Jérôme, *Carbohydr. Polym.*, 2011, **86**, 1093–1106.
75 Y. Zhang, J. W. Chan, A. Moretti and K. E. Uhrich, *J. Controlled Release*, 2015, **219**, 355–368.
76 M. V. Liberti and J. W. Lacosale, *Trends Biochem. Sci.*, 2016, **41**, 211–218.
77 O. Warburg, *J. Cancer Res.*, 1925, **9**, 148–163.
78 O. Warburg, *Science*, 1956, **123**, 309–314.
79 K. Sato, K. Yoshida, S. Takahashi and J. Anzai, *Adv. Drug Delivery Rev.*, 2011, **63**, 809–821.
80 W. Chen, Y. Zou, F. Meng, R. Cheng, C. Deng, J. Feijen and Z. Zhong, *Biomacromolecules*, 2014, **15**, 900–907.
81 Y. C. Lee and R. T. Lee, *Acc. Chem. Res.*, 1995, **28**, 321–327.
82 A. David, P. Kopecková, J. Kopecek and A. Rubinstein, *Pharm. Res.*, 2002, **19**, 1114–1122.
83 N. Jayaraman, *Chem. Soc. Rev.*, 2009, **38**, 3463–3483.
84 C. R. Becer, *Macromol. Rapid Commun.*, 2012, **33**, 742–752.
85 F. Demir Duman, A. Monaco, R. Foulkes, C. R. Becer and R. S. Forgan, *ACS Appl. Nano Mater.*, 2022, **5**, 13862–13873.
86 K. Lu, Y. Qu, Y. Lin, L. Li, Y. Wu, Y. Zou, T. Chang, Y. Zhang, Q. Yu and H. Chen, *ACS Appl. Mater. Interfaces*, 2022, **14**, 2618–2628.
87 P. S. Omurtag Ozgen, S. Atasoy, B. Zengin Kurt, Z. Durmus, G. Yigit and A. Dag, *J. Mater. Chem. B*, 2020, **8**, 3123–3137.
88 N. Ding, S. Xu, S. Zheng, Q. Ye, L. Xu, S. Ling, S. Xie, W. Chen, Z. Zhang, M. Xue, Z. Lin, X. Xu and L. Wang, *J. Mater. Chem. B*, 2021, **9**, 2816–2830.
89 Y. Song, M. Elsabahy, C. A. Collins, S. Khan, R. Li, T. N. Hreha, Y. Shen, Y.-N. Lin, R. A. Letteri, L. Su, M. Dong, F. Zhang, D. A. Hunstad and K. L. Wooley, *Nano Lett.*, 2021, **21**, 4990–4998.

 This journal is © The Royal Society of Chemistry 2026

Open Access Article. Published on 24 November 2025. Downloaded on 6/6/2026 1:27:29 AM. This article is licensed under a Creative Commons Attribution-NonCommercial 3.0 Unported Licence.

90 N. Lecot, M. Fernández-Lomónaco, H. Cerecetto, J. P. Gambini, P. Cabral and R. Glisoni, *RSC Pharm.*, 2024, **1**, 57–67.
91 K. M. Zepon, I. Otsuka, C. Bouilhac, E. C. Muniz, V. Soldi and R. Borsali, *Biomacromolecules*, 2015, **16**, 2012–2024.
92 J. Niu, L. Wang, M. Yuan, J. Zhang, H. Chen and Y. Zhang, *J. Drug Delivery Sci. Technol.*, 2020, **57**, 101343.
93 Y. Yin, J. Wang, M. Yang, R. Du, G. Pontrelli, S. McGinty, G. Wang, T. Yin and Y. Wang, *Nanoscale*, 2020, **12**, 2946–2960.
94 M. H. Stenzel, *Macromolecules*, 2022, **55**, 4867–4890.
95 S. Parcero-Bouzas, J. Correa, C. Jimenez-Lopez, B. D. Gonzalez and E. Fernandez-Megia, *Biomacromolecules*, 2024, **25**, 2780–2791.
96 R. Wang, G.-T. Chen, F.-S. Du and Z.-C. Li, *Colloids Surf., B*, 2011, **85**, 56–62.
97 R.-S. Lee and K.-Y. Peng, *React. Funct. Polym.*, 2012, **72**, 564–573.
98 K.-Y. Peng, M.-Y. Hua and R.-S. Lee, *Carbohydr. Polym.*, 2014, **99**, 710–719.
99 A. G. D. Bó, V. Soldi, F. C. Giacomelli, C. Travelet, R. Borsali and S. Fort, *Carbohydr. Res.*, 2014, **397**, 31–36.
100 M. Sakashita, S. Mochizuki and K. Sakurai, *Bioorg. Med. Chem.*, 2014, **22**, 5212–5219.
101 L. Yin, Y. Chen, Z. Zhang, Q. Yin, N. Zheng and J. Cheng, *Macromol. Rapid Commun.*, 2015, **36**, 483–489.
102 T. E. A. Frizon, Y. M. S. Micheletto, J. L. Westrup, P. S. S. Wakabayashi, F. R. Serafim, A. P. Damiani, L. M. Longaretti, V. M. de Andrade, F. C. Giacomelli, S. Fort and A. G. D. Bó, *Colloids Surf., B*, 2015, **133**, 323–330.
103 X. Zhou, X. Qin, T. Gong, Z.-R. Zhang and Y. Fu, *Macromol. Biosci.*, 2017, **17**, 1600529.
104 A. G. D. Bó, V. Soldi, F. C. Giacomelli, C. Travelet, B. Jean, I. Pignot-Paintrand, R. Borsali and S. Fort, *Langmuir*, 2012, **28**, 1418–1426.
105 M. Assali, J.-J. Cid, I. Fernández and N. Khiar, *Chem. Mater.*, 2013, **25**, 4250–4261.
106 S.-H. Kim, J.-H. Kim, D. G. You, G. Saravanakumar, H. Y. Yoon, K. Y. Choi, T. Thambi, V. G. Deepagan, D.-G. Jo and J. H. Park, *Chem. Commun.*, 2013, **49**, 10349–10351.
107 S. S.-S. Wang, S.-C. How, Y.-D. Chen, Y.-H. Tsaic and J.-S. Jan, *J. Mater. Chem. B*, 2015, **3**, 5220–5231.
108 S. S. Yu, C. M. Lau, W. J. Barham, H. M. Onishko, C. E. Nelson, H. Li, C. A. Smith, F. E. Yull, C. L. Duvall and T. D. Giorgio, *Mol. Pharmaceutics*, 2013, **10**, 975–987.
109 M. Hetzer, G. Chen, C. Barner-Kowolik and M. H. Stenzel, *Macromol. Biosci.*, 2010, **10**, 119–126.
110 K. Babiuch, A. Dag, J. Zhao, H. Lu and M. H. Stenzel, *Biomacromolecules*, 2015, **16**, 1948–1957.
111 J. R. Kramer and T. J. Deming, *Polym. Chem.*, 2014, **5**, 671–682.
112 J. Huang, C. Bonduelle, J. Thévenot, S. Lecommandoux and A. Heise, *J. Am. Chem. Soc.*, 2012, **134**, 119–122.
113 C. Gauche and S. Lecommandoux, *Polymer*, 2016, **107**, 474–484.
114 D. Pati, N. Kalva, S. Das, G. Kumaraswamy, S. S. Gupta and A. V. Ambade, *J. Am. Chem. Soc.*, 2012, **134**, 7796–7802.
115 V. Dhaware, A. Y. Shaikh, M. Kar, S. Hotha and S. S. Gupta, *Langmuir*, 2013, **29**, 5659–5667.
116 C. Bonduelle, J. Huang, T. Mena-Barragán, C. O. Mellet, C. Decroocq, E. Etamé, A. Heise, P. Compain and S. Lecommandoux, *Chem. Commun.*, 2014, **50**, 3350–3352.
117 H.-K. Yang, J.-F. Bao, L. Mo, R.-M. Yang, X.-D. Xu, W.-J. Tang, J.-T. Lin, G.-H. Wang, L.-M. Zhang and X.-Q. Jiang, *RSC Adv.*, 2017, **7**, 21093–21106.
118 A. L. Martin, B. Li and E. R. Gillies, *J. Am. Chem. Soc.*, 2009, **131**, 734–741.
119 D.-D. Chang, W.-H. Yang, X.-H. Dai, J.-X. Wang, L. Chen, J.-M. Pan, Y.-S. Yan and Y.-R. Dai, *J. Polym. Res.*, 2018, **25**, 257.
120 L. Sun, Y. Yang, C.-M. Dong and Y. Wei, *Small*, 2011, **7**, 401–406.
121 T. Isono, K. Miyachi, Y. Satoh, R. Nakamura, Y. Zhang, I. Otsuka, K. Tajima, T. Kakuchi, R. Borsali and T. Satoh, *Macromolecules*, 2016, **49**, 4178–4194.
122 Y.-Y. Guo, B. Zhang, L. Wang, S. Huang, S. Wang, Y. You, G. Zhu, A. Zhu, M. Geng and L. Li, *Chem. Commun.*, 2020, **56**, 14401–14403.
123 A. K. Agrahari, P. Bose, M. K. Jaiswal, S. Rajkhowa, A. S. Singh, S. Hotha, N. Mishra and V. K. Tiwari, *Chem. Rev.*, 2021, **121**, 7638–7956.
124 M. M. Kose, S. Onbulak, I. I. Yılmaz and A. Sanyal, *Macromolecules*, 2011, **44**, 2707–2714.
125 V. Cedrati, A. Pacini, A. Nitti, A. M. de Ilarduya, S. Munoz-Guerra, A. Sanyal and D. Pasini, *Polym. Chem.*, 2020, **11**, 5582–5589.
126 S. Luleburgaz, E. Cakmakci, H. Durmaz and U. Tunca, *Eur. Polym. J.*, 2024, **209**, 112897.
127 C. E. Hoyle and C. N. Bowman, *Angew. Chem., Int. Ed.*, 2010, **49**, 1540–1573.
128 A. B. Lowe, C. E. Hoyle and C. N. Bowman, *J. Mater. Chem.*, 2010, **20**, 4745–4750.
129 E. Kim and H. Koo, *Chem. Sci.*, 2019, **10**, 7835–7851.
130 J. Kumar, A. Bousquet and M. H. Stenzel, *Macromol. Rapid Commun.*, 2011, **32**, 1620–1626.
131 C. Chen, H. Xu, Y.-C. Qiana and X.-J. Huang, *RSC Adv.*, 2015, **5**, 15909–15915.
132 N. Kaur, P. Popli, N. Tiwary and R. Swami, *J. Controlled Release*, 2023, **355**, 417–433.
133 G. L. Zwicke, G. A. Mansoori and C. J. Jeffery, *Nano Rev.*, 2012, **3**, 18496.
134 X. Jin, J. Zhang, X. Jin, L. Liu and X. Tian, *ACS Med. Chem. Lett.*, 2020, **11**, 1514–1520.
135 L. Fan, J. Wang, C. Xia, Q. Zhang, Y. Pu, L. Chen, J. Chen and Y. Wang, *J. Mater. Chem. B*, 2020, **8**, 3113–3122.
136 G. Birlik Demirel, E. Aygul, A. Dag, S. Atasoy, Z. Cimen and B. Cetin, *ACS Appl. Bio Mater.*, 2020, **3**, 4949–4961.
137 D. Wang, Z. Fan, X. Zhang, H. Li, Y. Sun, M. Cao, G. Wei and J. Wang, *Langmuir*, 2021, **37**, 339–347.
138 C. Rizzo, P. Cancemi, M. Buttacavoli, G. Di Cara, C. D'Amico, F. Billeci, S. Marullo and F. D'Anna, *J. Mater. Chem. B*, 2023, **11**, 7721–7738.

Open Access Article. Published on 24 November 2025. Downloaded on 6/6/2026 1:27:29 AM. This article is licensed under a Creative Commons Attribution-NonCommercial 3.0 Unported Licence.

139 B. H. Ali, S. Khoee, F. Mafakheri, E. Sadri, V. P. Mahabadi, M. R. Karimi, S. Shirvalilou and S. Khoei, *J. Mater. Chem. B*, 2024, **12**, 5957–5973.
140 J. Yu, X. Xie, X. Xu, L. Zhang, X. Zhou, H. Yu, P. Wu, T. Wang, X. Che and Z. Hua, *J. Mater. Chem. B*, 2014, **2**, 2114–2126.
141 S. Panja, G. Dey, R. Bharti, K. Kumari, T. K. Maiti, M. Mandal and S. Chattopadhyay, *ACS Appl. Mater. Interfaces*, 2016, **8**, 12063–12074.
142 Q. Lu, M. Yi, M. Zhang, Z. Shi and S. Zhang, *Langmuir*, 2019, **35**, 504–512.
143 L. Jiang, Z.-m Gao, L. Ye, A.-y Zhang and Z.-g Feng, *Polymer*, 2013, **54**, 5188–5198.
144 M. Wang, J. Long, S. Zhang, F. Liu, X. Zhang, X. Zhang, L. Sun, L. Ma, C. Yu and H. Wei, *ACS Biomater. Sci. Eng.*, 2020, **6**, 1565–1572.
145 W. Du, Q. Lu, M. Zhang, H. Cao and S. Zhang, *ACS Appl. Bio Mater.*, 2021, **4**, 3246–3255.
146 J. Wei, X. Shuai, R. Wang, X. He, Y. Li, M. Ding, J. Li, H. Tan and Q. Fu, *Biomaterials*, 2017, **145**, 138–153.
147 K. Halama, M. T.-Y. Lin, A. Schaffer, M. Foith, F. Adams and B. Rieger, *Macromolecules*, 2024, **57**, 1438–1447.
148 T. Liu, Y. Qian, X. Hu, Z. Ge and S. Liu, *J. Mater. Chem.*, 2012, **22**, 5020–5030.
149 X. Hu, J. Tian, T. Liu, G. Zhang and S. Liu, *Macromolecules*, 2013, **46**, 6243–6256.
150 N. Song, M. Ding, Z. Pan, J. Li, L. Zhou, H. Tan and Q. Fu, *Biomacromolecules*, 2013, **14**, 4407–4419.
151 C.-C. Cheng, S.-Y. Huang, W.-L. Fan, A.-W. Lee, C.-W. Chiu, D.-J. Lee and J.-Y. Lai, *ACS Appl. Polym. Mater.*, 2021, **3**, 474–484.
152 B. Purushothaman, J. Choi, S. Park, J. Lee, A. A. S. Samson, S. Honga and J. M. Song, *J. Mater. Chem. B*, 2019, **7**, 65–79.
153 B. K. Kundu, S. Singh, W. A. C. Ranjith, S. Sarkar, A. Sonawane and S. Mukhopadhyay, *ACS Appl. Mater. Interfaces*, 2023, **15**, 43345–43358.
154 X. Jiang, S. Liu and R. Narain, *Langmuir*, 2009, **25**, 13344–13350.
155 L. Chan, Y. Huang and T. Chen, *J. Mater. Chem. B*, 2016, **4**, 4517–4525.
156 Y. Singh, K. K. D. R. Viswanadham, A. K. Jajoriya, J. G. Meher, K. Raval, S. Jaiswal, J. Dewangan, H. K. Bora, S. K. Rath, J. Lal, D. P. Mishra and M. K. Chourasia, *Mol. Pharmaceutics*, 2017, **14**, 2749–2765.
157 S. Ilyas, N. K. Ullah, M. Ilyas, K. Wennhold, M. Iqbal, H. A. Schlößer, M. S. Hussain and S. Mathur, *ACS Biomater. Sci. Eng.*, 2020, **6**, 6138–6147.
158 W. Lv, L. Liu, Y. Luo, X. Wang and Y. Liu, *J. Colloid Interface Sci.*, 2011, **356**, 16–23.
159 F. Fang, J. Liu, Y. Li, J. Yang and J. Yang, *Macromol. Biosci.*, 2018, **18**, 1700392.
160 A. Doerflinger, N. N. Quang, E. Gravel, G. Pinna, M. Vandamme, F. Ducongé and E. Doris, *Chem. Commun.*, 2018, **54**, 3613–3616.
161 I. Pretzer, D. Bushiri and R. Weberskirch, *Macromol. Mater. Eng.*, 2023, **308**, 2200627.
162 J. Jin, D. Wu, P. Sun, L. Liu and H. Zhao, *Macromolecules*, 2011, **44**, 2016–2024.
163 M. Roveri, M. Bernasconi, J.-C. Leroux and P. Luciani, *J. Mater. Chem. B*, 2017, **5**, 4348–4364.
164 Z. Jiang, J. Guan, J. Qian and C. Zhan, *Biomater. Sci.*, 2019, **7**, 461–471.
165 L. Sun, H. Liu, Y. Ye, Y. Lei, R. Islam, S. Tan, R. Tong, Y.-B. Miao and L. Cai, *Signal Transduction Targeted Ther.*, 2023, **8**, 418.
166 A. Degirmenci, R. Sanyal, H.-A. Klok and A. Sanyal, *J. Am. Chem. Soc.*, 2025, **147**, 24672–24683.
167 N. Ejderyan, M. G. Bilgin, S. Kocak, R. Sanyal and A. Sanyal, *Eur. Polym. J.*, 2025, **238**, 114207.
168 Y. Wang, W. Shi, W. Song, L. Wang, X. Liu, J. Chen and R. Huang, *J. Mater. Chem.*, 2012, **22**, 14608–14616.
169 P. Das, I. Pan, E. Cohen and M. Reches, *J. Mater. Chem. B*, 2018, **6**, 8228–8237.
170 N. Zhang, C. Lu, G. Shu, J. Li, M. Chen, C. Chen, X. Lv, X. Xu, W. Weng, Q. Weng, B. Tang, Y.-Z. D and J. Ji, *Biomater. Sci.*, 2020, **8**, 1961–1972.
171 S. M. Vasudevan, N. Ashwanikumarc and G. S. V. Kumar, *Biomater. Sci.*, 2019, **7**, 4017–4021.
172 J. Li, Y.-J. Wei, X.-L. Yang, W.-X. Wu, M.-Q. Zhang, M.-Y. Li, Z.-E. Hu, Y.-H. Liu, N. Wang and X.-Q. Yu, *ACS Appl. Mater. Interfaces*, 2020, **12**, 32432–32445.
173 N. N. Bayram, G. T. Ulu, M. Topuzoğulları, Y. Baran and S. Dincer İsoğlu, *Macromol. Biosci.*, 2022, **22**, 2100375.
174 I. M. Paiva, M. R. Vakili, A. H. Soleimani, S. A. T. Dakhili, S. Munira, M. Paladino, G. Martin, F. R. Jirik, D. G. Hall, M. Weinfeld and A. Lavasanifar, *Mol. Pharmaceutics*, 2022, **19**, 1825–1838.
175 M. Zhao, Y. Liu, R. S. Hsieh, N. Wang, W. Tai, K. Joo, P. Wang, Z. Gu and Y. Tang, *J. Am. Chem. Soc.*, 2014, **136**, 15319–15325.
176 J. Wan, A. Brust, R. F. Bhola, P. Jha, M. Mobli, R. J. Lewis, M. J. Christie and P. F. Alewood, *J. Pept. Sci.*, 2016, **22**, 280–289.
177 S. Tima, S. Okonogi, C. Ampasavate, C. Pickens, C. Berkland and S. Anuchapreeda, *J. Pharm. Sci.*, 2016, **105**, 3645–3657.
178 G. Jia, Y. Han, Y. An, Y. Ding, C. He, X. Wang and Q. Tang, *Biomaterials*, 2018, **178**, 302–316.
179 K. Xiao, Y. Li, J. S. Lee, A. M. Gonik, T. Dong, G. Fung, E. Sanchez, L. Xing, H. R. Cheng, J. Luo and K. S. Lam, *Cancer Res.*, 2012, **72**, 2100–2110.
180 S.-S. Han, Z.-Y. Li, J.-Y. Zhu, K. Han, Z.-Y. Zeng, W. Hong, W.-X. Li, H.-Z. Jia, Y. Liu, R.-X. Zhuo and X.-Z. Zhang, *Small*, 2015, **11**, 2543–2554.
181 Y. Lu, Z. Guo, Y. Zhang, C. Li, Y. Zhang, Q. Guo, Q. Chen, X. Chen, X. He, L. Liu, C. Ruan, T. Sun, B. Ji, W. Lu and C. Jiang, *Adv. Sci.*, 2019, **6**, 1801586.
182 Z. Han, Z. Li, R. Raveendran, S. Farazi, C. Cao, R. Chapman and M. H. Stenzel, *Biomacromolecules*, 2023, **24**, 5046–5057.
183 P. Zhang, L. Hu, Q. Yin, Z. Zhang, L. Feng and Y. Li, *J. Controlled Release*, 2012, **159**, 429–434.

 This journal is © The Royal Society of Chemistry 2026

Open Access Article. Published on 24 November 2025. Downloaded on 6/6/2026 1:27:29 AM. This article is licensed under a Creative Commons Attribution-NonCommercial 3.0 Unported Licence.

184 Y. Qian, Y. Zha, B. Feng, Z. Pang, B. Zhang, X. Sun, J. Ren, C. Zhang, X. Shao, Q. Zhang and X. Jiang, *Biomaterials*, 2013, **34**, 2117–2129.
185 W. T. Li, J. R. Peng, L. W. Tan, J. Wu, K. Shi, Y. Qu, X. W. Wei and Z. Y. Qian, *Biomaterials*, 2016, **106**, 119–133.
186 Y. Cai, Z. Xu, Q. Shuai, F. Zhu, J. Xu, X. Gao and X. Sun, *Biomater. Sci.*, 2020, **8**, 2274–2282.
187 Z. Guo, J. Sui, Y. Li, Q. Wei, C. Wei, L. Xiu, R. Zhu, Y. Sun, J. Hu and J.-L. Li, *J. Mater. Chem. B*, 2022, **10**, 9266–9279.
188 R. J. Passarella, D. E. Spratt, A. E. van der Ende, J. G. Phillips, H. Wu, V. Sathiyakumar, L. Zhou, D. E. Hallahan, E. Harth and R. Diaz, *Cancer Res.*, 2010, **70**, 4550–4559.
189 X. Hao, Q. Li, J. Lv, L. Yu, X. Ren, L. Zhang, Y. Feng and W. Zhang, *ACS Appl. Mater. Interfaces*, 2015, **7**, 12128–12140.
190 S. M. Garg, I. M. Paiva, M. R. Vakili, R. Soudy, K. Agopsowicz, A. H. Soleimani, M. Hitt, K. Kaur and A. Lavasanifar, *Biomaterials*, 2017, **144**, 17–29.
191 H. Kakwere, E. S. Ingham, R. Allen, L. M. Mahakian, S. M. Tam, H. Zhang, M. T. Silvestrini, J. S. Lewis and K. W. Ferrara, *Biomater. Sci.*, 2018, **6**, 2850–2858.
192 F. Danhier, A. Le Breton and V. Préat, *Mol. Pharmaceutics*, 2012, **9**, 2961–2973.
193 H. Javid, M. A. Oryani, N. Rezagholinejad, A. Esparham, M. Tajaldini and M. Karimi-Shahri, *Cancer Med.*, 2024, **13**, e6800.
194 M. Oba, K. Aoyagi, K. Miyata, Y. Matsumoto, K. Itaka, N. Nishiyama, Y. Yamasaki, H. Koyama and K. Kataoka, *Mol. Pharmaceutics*, 2008, **5**, 1080–1092.
195 L. Lu, X. Zhao, T. Fu, K. Li, Y. He, Z. Luo, L. Dai, R. Zeng and K. Cai, *Biomaterials*, 2020, **230**, 119666.
196 Y.-J. Cheng, S.-Y. Qin, W.-L. Liu, Y.-H. Ma, X.-S. Chen, A.-Q. Zhang and X.-Z. Zhang, *Adv. Mater. Interfaces*, 2020, **7**, 2000935.
197 Z. Zhang, Z. Lu, Q. Yuan, C. Zhang and Y. Tang, *J. Mater. Chem. B*, 2021, **9**, 2240–2248.
198 B. Cengiz, I. I. Demiralp, A. Degirmenci, N. Ejderyan, R. Sanyal and A. Sanyal, *ACS Appl. Polym. Mater.*, 2025, **7**, 12500–12509.
199 Y. Zhang, F. Huang, C. Ren, L. Yang, J. Liu, Z. Cheng, L. Chu and J. Liu, *ACS Appl. Mater. Interfaces*, 2017, **9**, 13016–13028.
200 L. Chambre, A. Degirmenci, R. Sanyal and A. Sanyal, *Bioconjugate Chem.*, 2018, **29**, 1885–1896.
201 J. Yan, B. Gundsambuu, M. Krasowska, K. Platts, P. F. Marina, C. Gerber, S. C. Barry and A. Blencowe, *J. Mater. Chem. B*, 2022, **10**, 3329–3343.
202 C.-Y. Huang, C.-Y. Chen, C.-H. Wei, J.-W. Yang, Y.-C. Lin, C.-F. Kao, J. H. Y. Chung and G.-Y. Chen, *J. Mater. Chem. B*, 2024, **12**, 8733–8745.
203 W. Ke, Z. Zha, J. F. Mukerabigwi, W. Chen, Y. Wang, C. He and Z. Ge, *Bioconjugate Chem.*, 2017, **28**, 2190–2198.
204 R. Zhou, M. Zhang, J. He, J. Liu, X. Sun and P. Ni, *ACS Omega*, 2022, **7**, 21325–21336.
205 C. Zhan, B. Gu, C. Xie, J. Li, Y. Liu and W. Lu, *J. Controlled Release*, 2010, **143**, 136–142.
206 Y. Miura, T. Takenaka, K. Toh, S. Wu, H. Nishihara, M. R. Kano, Y. Ino, T. Nomoto, Y. Matsumoto, H. Koyama, H. Cabral, N. Nishiyama and K. Kataoka, *ACS Nano*, 2013, **7**, 8583–8592.
207 C. Guojun, W. Liwei, C. Travis, V. Corinne, E. Kevin and W. G. Shaoqin, *Biomaterials*, 2015, **47**, 41–50.
208 Y. Lei, S. Chen, X. Zeng, Y. Meng, C. Chang and G. Zheng, *J. Appl. Polym. Sci.*, 2022, **139**, 52358.
209 F. Xiaoshan, Z. Weiwei, H. Zhiguo and L. Zibiao, *J. Mater. Chem. B*, 2017, **5**, 1062–1072.
210 S. Xue, X. Gu, J. Zhang, H. Sun, C. Deng and Z. Zhong, *Biomacromolecules*, 2018, **19**, 3586–3593.
211 J. Guo, G. Chen, X. Ning, M. A. Wolfert, X. Li, B. Xu and G.-J. Boons, *Chem. – Eur. J.*, 2010, **16**, 13360–13366.
212 T. Valero, A. Delgado-González, J. D. Unciti-Broceta, V. Cano-Cortés, A. M. Pérez-López, A. Unciti-Broceta and R. M. Sánchez Martín, *Bioconjugate Chem.*, 2018, **29**, 3154–3160.
213 F. Chen, Z. Jia, K. C. Rice, R. A. Reinhardt, K. W. Bayles and D. Wang, *Pharm. Res.*, 2013, **30**, 2808–2817.
214 X. Pei, F. Luo, J. Zhang, W. Chen, C. Jiang and J. Liu, *Sci. Rep.*, 2017, **7**, 975.
215 Y. Gao, H. Zhang, Y. Zhang, T. Lv, L. Zhang, Z. Li, X. Xie, F. Li, H. Chen and L. Jia, *Mol. Pharmaceutics*, 2018, **15**, 5146–5161.
216 Y. Zhang, P. Lundberg, M. Diether, C. Porsch, C. Janson, N. A. Lynd, C. Ducani, M. Malkoch, E. Malmström, C. J. Hawker and A. M. Nyström, *J. Mater. Chem. B*, 2015, **3**, 2472–2486.
217 X. Lu, X. Wan, J. Lian, J. Peng, P. Jing, Q. Guo, Y. Liao, Y. Jiang, C. Yang, L. Jin, S. Shi, Y. Yao, W. (Walter) Hu and J. Luo, *J. Colloid Interface Sci.*, 2025, **685**, 648–660.
218 S. Zhao, F. Chen, X. Chen, H. Liang, H. Tan and L. Zhao, *ACS Appl. Nano Mater.*, 2024, **7**, 26813–26824.
219 S. Li, K. Hu, W. Cao, Y. Sun, W. Sheng, F. Li, Y. Wu and X.-J. Liang, *Nanoscale*, 2014, **6**, 13701–13709.
220 N. Yoshinaga, T. Miyamoto, M. Goto, A. Tanaka and K. Numata, *JACS Au*, 2024, **4**, 1385–1395.
221 H. O. Alsaab, S. Sau, R. M. Alzhrani, V. T. Cheriyan, L. A. Polin, U. Vaishampayan, A. K. Rishi and A. K. Iyer, *Biomaterials*, 2018, **183**, 280–294.
222 G. Köhler and C. Milstein, *Nature*, 1975, **256**, 495–497.
223 S. L. Morrison, M. J. Johnson, L. A. Herzenberg and V. T. Oi, *Proc. Natl. Acad. Sci. U. S. A.*, 1984, **81**, 6851–6855.
224 P. Jones, P. Dear, J. Foote, M. S. Neuberger and G. Winter, *Nature*, 1986, **321**, 522–525.
225 C. Queen, W. P. Schneider, H. E. Selick, P. W. Payne, N. F. Landolfi, J. F. Duncan, N. M. Avdalovic, M. Levitt, R. P. Junghans and T. A. Waldmann, *Proc. Natl. Acad. Sci. U. S. A.*, 1989, **86**, 10029–10033.
226 L. Qian, X. Lin, X. Gao, R. U. Khan, J.-Y. Liao, S. Du, J. Ge, S. Zeng and S. Q. Yao, *Chem. Rev.*, 2023, **123**, 7782–7853.
227 J. K. McGavin and C. M. Spencer, *Drugs*, 2001, **61**, 1317–1322.
228 J. M. Lambert and R. V. J. Chari, *J. Med. Chem.*, 2014, **57**, 6949–6964.

Open Access Article. Published on 24 November 2025. Downloaded on 6/6/2026 1:27:29 AM. This article is licensed under a Creative Commons Attribution-NonCommercial 3.0 Unported Licence.

229 S. Tsuboia and T. Jin, *RSC Adv.*, 2020, **10**, 28171–28179.
230 W. Lee, K. N. Bobba, J. Y. Kim, H. Park, A. Bhise, W. Kim, K. Lee, S. Rajkumar, B. Nam, K. C. Lee, S. H. Lee, S. Ko de, H. J. Lee, S. T. Jung de and J. Yoo, *J. Mater. Chem. B*, 2021, **9**, 2993–2997.
231 P. Grossenbacher, M. C. Essersa, J. Moserb, S. A. Singera, S. Häusler, B. Stieger, J.-S. Rougiera and M. Lochner, *RSC Adv.*, 2022, **12**, 28306–28317.
232 J. Xiao, S. Qiu, Q. Ma, S. Bai, X. Guo and L. Wang, *J. Mater. Chem. B*, 2023, **11**, 10738–10746.
233 B. Hoang, S. N. Ekdawi, R. M. Reilly and C. Allen, *Mol. Pharmaceutics*, 2013, **10**, 4229–4241.
234 A. C. Hortelão, R. Carrascosa, N. Murillo-Cremaes, T. Patiño and S. Sánchez, *ACS Nano*, 2019, **13**(1), 429–439.
235 X. Ma, Z. Zhao, H. Wang, Y. Liu, Y. Xu, J. Zhang, B. Chen, L. Li and Y. Zhao, *Adv. Healthcare Mater.*, 2019, **8**(13), 1900136.
236 W. Nie, G. Wu, J. Zhang, L.-L. Huang, J. Ding, A. Jiang, Y. Zhang, Y. Liu, J. Li, K. Pu and H.-Y. Xie, *Angew. Chem., Int. Ed.*, 2019, **59**, 2018–2022.
237 S. Liang, M. Sun, Y. Lu, S. Shi, Y. Yang, Y. Lin, C. Feng, J. Liu and C. Dong, *J. Mater. Chem. B*, 2020, **8**, 8368–8382.
238 H. Tian, Y. Huang, J. He, M. Zhang and P. Ni, *ACS Appl. Bio Mater.*, 2021, **4**, 4422–4431.
239 M. H. Mohd-Zahid, S. N. Zulkifli, C. A. C. Abdullah, J. K. Lim, S. Fakurazi, K. K. Wong, A. D. Zakaria, N. Ismail, V. Uskoković, R. Mohamud and Z. A. Iskandar, *RSC Adv.*, 2021, **11**, 16131–16141.
240 X. Zhang, P. Wei, Z. Wang, Y. Zhao, W. Xiao, Y. Bian, D. Liang, Q. Lin, W. Song, W. Jiang and H. Wang, *ACS Appl. Mater. Interfaces*, 2022, **14**, 15956–15969.
241 Y. J. Chae, K.-G. Lee, D. Oh, S.-K. Lee, Y. Park and J. Kim, *Adv. Healthcare Mater.*, 2024, **13**(19), 2400235.
242 Z. Zhou, A. Badkas, M. Stevenson, J.-Y. Lee and Y.-K. Leung, *Int. J. Pharm.*, 2015, **487**, 81–90.
243 M. Marcinkowska, M. Stanczyk, A. Janaszewska, E. Sobierajska, A. Chworos and B. Klajnert-Maculewicz, *Pharm. Res.*, 2019, **36**, 154.
244 P. Kanjilal, K. Singh, R. Das, J. Matte and S. Thayumanavan, *Biomacromolecules*, 2023, **24**(8), 3638–3646.
245 A. Creamer, A. L. Fiego, A. Agliano, L. Prados-Martin, H. Høgset, A. Najer, D. A. Richards, J. P. Wojciechowski, J. E. J. Foote, N. Kim, A. Monahan, J. Tang, A. Shamsabadi, L. N. C. Rochet, I. A. Thanasi, L. R. de la Ballina, C. L. Rapley, S. Turnock, E. A. Love, L. Bugeon, M. J. Dallman, M. Heeney, G. Kramer-Marek, V. Chudasama, F. Fenaroli and M. M. Stevens, *Adv. Mater.*, 2024, **36**, 2300413.
246 S. Gong, B. Liu, J. Qiu, F. Huang and S. Thayumanavan, *Small*, 2024, **20**, 2402874.
247 V. P. Torchilin, A. N. Lukyanov, Z. Gao and B. Papahadjopoulos-Sternberg, *Proc. Natl. Acad. Sci. U. S. A.*, 2003, **100**, 6039–6044.
248 R. R. Sawant, A. M. Jhaveri and V. P. Torchilin, *Adv. Drug Delivery Rev.*, 2012, **64**, 1436–1446.
249 T. Watanabe, H. L. Mizuno, J. Norimatsu, T. Obara, H. Cabral, K. Tsumoto, M. Nakakido, D. Kawauchi and Y. Anraku, *Polymers*, 2023, **15**, 1808.
250 P. Kumar, S.-H. Kim, S. Yadav, S.-H. Jo, S. Yoo II, S.-H. Park and K. T. Lim, *ACS Appl. Mater. Interfaces*, 2023, **15**, 12719–12734.
251 D. P. Y. Chan, G. F. Deleavey, S. C. Owen, M. J. Damha and M. S. Shoichet, *Biomaterials*, 2013, **34**, 8408–8415.
252 D. P. Y. Chan, S. C. Owen and M. S. Shoichet, *Bioconjugate Chem.*, 2013, **24**, 105–113.
253 J. Chen, A. Rizvi, J. P. Patterson and C. J. Hawker, *J. Am. Chem. Soc.*, 2022, **144**, 19466–19474.
254 S. Kramer, D. Svatunek, I. Alberg, B. Gräfen, S. Schmitt, L. Braun, A. H. A. M. van Onzen, R. Rossin, K. Koynov, H. Mikula and R. Zentel, *Biomacromolecules*, 2019, **20**, 3786–3797.
255 L. Chu, A. Wang, L. Ni, X. Yan, Y. Song, M. Zhao, K. Sun, H. Mu, S. Liu, Z. Wu and C. Zhang, *Drug Delivery*, 2018, **25**, 1634–1641.
256 K. Nishida, A. Tamura, T. W. Kang, H. Masuda and N. Yui, *J. Mater. Chem. B*, 2020, **8**, 6975–6987.
257 R. Chen, Y. Huang, L. Wang, J. Zhou, Y. Tan, C. Peng, P. Yang, W. Peng, J. Li, Q. Gu, Y. Sheng, Y. Wang, G. Shao, Q. Zhang and Y. Sun, *Biomater. Sci.*, 2021, **9**, 2279–2294.
258 J. Liu, G. Feng, D. Dinga and B. Liu, *Polym. Chem.*, 2013, **4**, 4326–4334.
259 X. Tang, L. Chen, A. Li, S. Cai, Y. Zhang, X. Liu, Z. Jiang, X. Liu, Y. Liang and D. Ma, *Drug Delivery*, 2018, **25**, 1484–1494.
260 Y.-H. Shih, T.-Y. Luo, P.-F. Chiang, C.-J. Yao, W.-J. Lin, C.-L. Peng and M.-J. Shieh, *J. Controlled Release*, 2017, **258**, 196–207.
261 H. Li, M. Zhang, J. He, J. Liu, X. Sun and P. Ni, *J. Mater. Chem. B*, 2023, **11**, 9467–9477.
262 J. Peng, J. Chen, F. Xie, W. Bao, H. Xu, H. Wang, Y. Xu and Z. Du, *Biomaterials*, 2019, **222**, 119420.
263 P. Chames, M. V. Regenmortel, E. Weiss and D. Baty, *Br. J. Pharmacol.*, 2009, **157**, 220–233.
264 K. T. Xenaki, S. Oliveira and P. M. P. van Bergen en Henegouwen, *Front. Immunol.*, 2017, **8**, 1287.
265 A. P. Chapman, P. Antoniw, M. Spitali, S. West, S. Stephens and D. J. King, *Nat. Biotechnol.*, 1999, **17**, 780–783.
266 J. Li and Z. Zhu, *Acta Pharmacol. Sin.*, 2010, **31**, 1198–1207.
267 Z.-R. Lu, J.-G. Shiah, S. Sakuma, P. Kopečková and J. Kopeček, *J. Controlled Release*, 2002, **78**, 165–173.
268 J. Hongrapipat, P. Kopečková, J. Liu, S. Prakongpan and J. Kopeček, *Mol. Pharmaceutics*, 2008, **5**, 696–709.
269 T.-W. Chu, J. Yang and J. Kopeček, *Biomaterials*, 2012, **33**, 7174–7181.
270 R. N. Johnson, P. Kopečková and J. Kopeček, *Biomacromolecules*, 2012, **13**, 727–735.
271 D. C. Radford, J. Yang, M. C. Doan, L. Li, A. S. Dixon, S. C. Owen and J. Kopeček, *J. Controlled Release*, 2020, **319**, 285–299.
272 T. Merdan, J. Callahan, H. Petersen, K. Kunath, U. Bakowsky, P. Kopečková, T. Kissel and J. Kopeček, *Bioconjugate Chem.*, 2003, **14**, 989–996.
273 D. I. Kang, S. Lee, J. T. Lee, B. J. Sung, J. Y. Yoon, J. K. Kim, J. Chung and S. J. Lim, *J. Microencapsulation*, 2011, **28**, 220–227.

 This journal is © The Royal Society of Chemistry 2026

Open Access Article. Published on 24 November 2025. Downloaded on 6/6/2026 1:27:29 AM. This article is licensed under a Creative Commons Attribution-NonCommercial 3.0 Unported Licence.

274 B. Hoang, R. M. Reilly and C. Allen, *Biomacromolecules*, 2012, **13**, 455–465.
275 W. W. K. Cheng and T. M. Allen, *J. Controlled Release*, 2008, **126**, 50–58.
276 M. Colombo, S. Sommaruga, S. Mazzucchelli, L. Polito, P. Verderio, P. Galeffi, F. Corsi, P. Tortora and D. Prosperi, *Angew. Chem., Int. Ed.*, 2012, **51**, 496–499.
277 L. Deng, Y. Zhang, L. Ma, X. Jing, X. Ke, J. Lian, Q. Zhao, B. Yan, J. Zhang, J. Yao and J. Chen, *Int. J. Nanomed.*, 2013, **8**, 3271–3283.
278 P. J. Kennedy, F. Sousa, D. Ferreira, C. Pereira, M. Nestor, C. Oliveira, P. L. Granja and B. Sarmento, *Acta Biomater.*, 2018, **81**, 208–218.
279 M. Darwish, W. Shatz, B. Leonard, K. Loyet, K. Barrett, J. L. Wong, H. Li, R. Abraham, M. Lin, Y. Franke, C. Tam, K. Mortara, I. Zilberleyb and C. Blanchette, *Bioconjugate Chem.*, 2020, **31**, 1995–2007.
280 K. Singh, M. Canakci, P. Kanjilal, N. Williams, S. Shanthalingam, B. A. Osborne and S. Thayumanavan, *Bioconjugate Chem.*, 2022, **33**, 486–495.
281 J. Ahn, Y. Miura, N. Yamada, T. Chida, X. Liu, A. Kim, R. Sato, R. Tsumura, Y. Koga, M. Yasunaga, N. Nishiyama, Y. Matsumura, H. Cabral and K. Kataoka, *Biomaterials*, 2015, **39**, 23–30.
282 Q. Ji, J. Hou, X. Yong, G. Gong, M. Muddassir, T. Tang, J. Xie, W. Fan and X. Chen, *Adv. Mater.*, 2021, **33**, 2007798.
283 J. Hou, Q. Ji, J. Ji, S. Ju, C. Xu, X. Yong, X. Xu, M. Muddassir, X. Chen, J. Xie and X. Han, *Theranostics*, 2021, **11**, 3244–3261.
284 S. Florinas, M. Liu, R. Fleming, L. V. Vlerken-Ysla, J. Ayriss, R. Gilbreth, N. Dimasi, C. Gao, H. Wu, Z.-Q. Xu, S. Chen, A. Dirisala, K. Kataoka, H. Cabral and R. J. Christie, *Biomacromolecules*, 2016, **17**, 1818–1833.
285 S. Chen, S. Florinas, A. Teitgen, Z.-Q. Xu, C. Gao, H. Wu, K. Kataoka, H. Cabral and R. J. Christie, *Sci. Technol. Adv. Mater.*, 2017, **18**, 666–680.
286 H. S. Min, H. J. Kim, J. Ahn, M. Naito, K. Hayashi, K. Toh, B. S. Kim, Y. Matsumura, I. C. Kwon, K. Miyata and K. Kataoka, *Biomacromolecules*, 2018, **19**, 2320–2329.
287 M. Shahdordizadeh, R. Yazdian-Robati, M. Ramezani, K. Abnous and S. M. Taghdisi, *J. Mater. Chem. B*, 2016, **4**, 7766–7778.
288 L. C. Bock, L. C. Griffin, J. A. Latham, E. H. Vermaas and J. J. Toole, *Nature*, 1992, **355**, 564–566.
289 S. Sekiya, F. Nishikawa, K. Fukuda and S. Nishikawa, *J. Biochem.*, 2003, **133**, 351–359.
290 C. Tuerk and L. Gold, *Science*, 1990, **249**, 505–510.
291 A. D. Ellington and J. W. Szostak, *Nature*, 1990, **346**, 818–822.
292 J.-H. Lee, M. D. Canny, A. De Erkenez, D. Krilleke, Y.-S. Ng, D. T. Shima, A. Pardi and F. Jucker, *Proc. Natl. Acad. Sci. U. S. A.*, 2005, **102**, 18902–18907.
293 H. Jo, H. Youn, S. Lee and C. Ban, *J. Mater. Chem. B*, 2014, **2**, 4862–4867.
294 Z. Fang, X. Wang, Y. Sun, R. Fan, Z. Liu, R. Guo and D. Xie, *Nanoscale*, 2019, **11**, 23000–23012.
295 Y. Liu, Y. Zou, C. Feng, A. Lee, J. Yin, R. Chung, J. B. Park, H. Rizos, W. Tao, M. Zheng, O. C. Farokhzad and B. Shi, *Nano Lett.*, 2020, **20**, 1637–1646.
296 S. Sanati, S. Taghavi, K. Abnous, S. M. Taghdisi, M. Babaei, M. Ramezani and M. Alibolandi, *Gene Ther.*, 2022, **29**, 55–68.
297 Y. Liu, W. Hou, H. Sun, C. Cui, L. Zhang, Y. Jiang, Y. Wu, Y. Wang, J. Li, B. S. Sumerlin, Q. Liu and W. Tan, *Chem. Sci.*, 2017, **8**, 6182–6187.
298 X. He, Q. Long, Z. Zeng, L. Yang, Y. Tang and X. Feng, *Adv. Funct. Mater.*, 2019, **29**, 1906187.
299 X. Liang, Y. Wang, H. Shi, M. Dong, H. Han and Q. Li, *Int. J. Nanomed.*, 2021, **16**, 2569–2584.
300 M. A. Harris, T. R. Pearce, T. Pengo, H. Kuang, C. Forster and E. Kokkoli, *Nanomed. Nanotechnol. Biol. Med.*, 2018, **14**, 85–96.
301 F. Xiao, L. Lin, Z. Chao, C. Shao, Z. Chen, Z. Wei, J. Lu, Y. Huang, L. Li, Q. Liu, Y. Liang and L. Tian, *Angew. Chem., Int. Ed.*, 2020, **59**, 9702–9710.
302 D. Wu, K. Yang, Z. Zhang, Y. Feng, L. Rao, X. Chen and G. Yu, *Chem. Soc. Rev.*, 2022, **51**, 1336–1376.
303 E. Saxon and C. R. Bertozzi, *Science*, 2000, **287**, 2007–2010.
304 J. M. Baskin, J. A. Prescher, S. T. Laughlin, N. J. Agard, P. V. Chang, I. A. Miller, A. Lo, J. A. Codelli and C. R. Bertozzi, *Proc. Natl. Acad. Sci. U. S. A.*, 2007, **104**, 16793–16797.
305 J. B. Haun, N. K. Devaraj, S. A. Hilderbrand, H. Lee and R. Weissleder, *Nat. Nanotechnol.*, 2010, **5**, 660–665.
306 S. S. Agasti, M. Liong, C. Tassa, H. J. Chung, S. Y. Shaw, H. Lee and R. Weissleder, *Angew. Chem., Int. Ed.*, 2012, **51**, 450–454.
307 S. Lee, S. Jung, H. Koo, J. H. Na, H. Y. Yoon, M. K. Shim, J. Park, J.-H. Kim, S. Lee, M. G. Pomper, I. C. Kwon, C. H. Ahn and K. Kim, *Biomaterials*, 2017, **148**, 1–15.
308 D. Mao, F. Hu, Kenry, S. Ji, W. Wu, D. Ding, D. Kong and B. Liu, *Adv. Mater.*, 2018, **30**, 1706831.
309 N. M. Meghani, H. H. Amin, C. Park, J.-B. Park, J.-H. Cui, Q.-R. Cao and B.-J. Lee, *Int. J. Pharm.*, 2018, **545**, 101–112.
310 J. Yoo, S. Choi, J. Son, G. Yi, E. Kim and H. Koo, *Biochem. Biophys. Res. Commun.*, 2019, **515**, 207–213.
311 Y. Tu, Y. Dong, K. Wang, S. Shen, Y. Yuan and J. Wang, *Biomaterials*, 2020, **259**, 120298.
312 L. Du, H. Qin, T. Ma, T. Zhang and D. Xing, *ACS Nano*, 2017, **11**, 8930–8943.
313 P. Zhang, X. Zhang, C. Li, S. Zhou, W. Wu and X. Jiang, *ACS Appl. Mater. Interfaces*, 2019, **11**, 32697–32705.
314 R. Wei, Y. Dong, Y. Tu, S. Luo, X. Pang, W. Zhang, W. Yao, W. Tang, H. Yang, X. Wei, X. Jiang, Y. Yuan and R. Yang, *ACS Appl. Mater. Interfaces*, 2021, **13**, 14004–14014.
315 Y. Li, M. Li, L. Liu, C. Xue, Y. Fei, X. Wang, Y. Zhang, K. Cai, Y. Zhao and Z. Luo, *ACS Nano*, 2022, **16**, 3965–3984.
316 S. Wang, Y. Zhang, Y. Wang, Y. Yang, S. Zhao, T. Sheng, Y. Zhang, Z. Gu, J. Wang and J. Yu, *Nat. Commun.*, 2023, **14**, 6953.

Open Access Article. Published on 24 November 2025. Downloaded on 6/6/2026 1:27:29 AM.
This article is licensed under a Creative Commons Attribution-NonCommercial 3.0 Unported Licence.

317 M. Deng, R. Guo, S. Zang, J. Rao, M. Li, X. Tang, C. Xia, M. Li, Z. Zhang and Q. He, *ACS Appl. Mater. Interfaces*, 2021, **13**, 18033–18046.
318 K. Wang, M. Jiang, J. Zhou, Y. Liu, Q. Zong and Y. Yuan, *ACS Nano*, 2022, **16**, 721–735.
319 O. Diels and K. Alder, *Justus Liebigs Ann. Chem.*, 1928, **460**, 98–122.
320 D. F. Rodríguez, Y. Moglie, C. A. Ramírez-Sarmiento, S. K. Singh, K. Dua and F. C. Zacconi, *RSC Adv.*, 2022, **12**, 1932–1949.
321 A. Oluwasanmi and C. Hoskins, *Int. J. Pharm.*, 2021, **604**, 120727.
322 S.-Y. Tang, J. Shi and Q.-X. Guo, *Org. Biomol. Chem.*, 2012, **10**, 2673–2682.
323 G. Wittig and A. Krebs, *Chem. Ber.*, 1961, **94**, 3260–3275.
324 N. J. Agard, J. A. Prescher and C. R. Bertozzi, *J. Am. Chem. Soc.*, 2004, **126**, 15046–15047.
325 P. Ramírez-López, J. R. Suárez, A. Flores and M. J. Hernáiz, *Bioconjugate Chem.*, 2025, **36**, 1553–1581.
326 D. Bauer, M. A. Cornejo, T. T. Hoang, J. S. Lewis and B. M. Zeglis, *Bioconjugate Chem.*, 2023, **34**, 1925–1950.
327 T. Deb, J. Tu and R. M. Franzini, *Chem. Rev.*, 2021, **121**, 6850–6914.
328 B. L. Oliveira, Z. Guo and G. J. L. Bernardes, *Chem. Soc. Rev.*, 2017, **46**, 4895–4950.
329 K. Shanbhag, K. Sharma and S. S. Kamat, *RSC Chem. Biol.*, 2023, **4**, 37–46.

 This journal is © The Royal Society of Chemistry 2026